environments

MDPI

Article

Seasonal and Spatial Variation of Stable Isotopic Composition of Precipitation in the Vardar River Basin, North Macedonia

Violeta Gjeshovska [1,*], Bojan Ilioski [1] and Zoran Kovač [2]

[1] Faculty of Civil Engineering Skopje, Ss. Cyril and Methodius University in Skopje, 1000 Skopje, North Macedonia; bilioski@gf.ukim.edu.mk
[2] Faculty of Mining, Geology and Petroleum Engineering, University of Zagreb, 10000 Zagreb, Croatia; zoran.kovac@rgn.unizg.hr
* Correspondence: violetag@gf.ukim.edu.mk

Abstract

This study investigates the seasonal and spatial variability of stable oxygen ($\delta^{18}O$) and hydrogen ($\delta^{2}H$) isotopes in precipitation within the Vardar River basin, North Macedonia, based on data collected from three monitoring stations between June 2025 and June 2026. The aim is to characterize temporal changes in isotopic composition, assess spatial differences between stations, and examine the relationships between isotope values and meteorological parameters, including air temperature, precipitation amount, relative humidity, wind speed, and atmospheric pressure. Building upon previous isotope-hydrological investigations in the basin, the study provides a more detailed assessment of precipitation isotope variability and its relationships with environmental conditions through seasonal analysis, evaluation of meteorological influences, and complementary spatial modelling approaches. The results reveal consistent isotopic depletion during winter and enrichment during summer at all three stations. Exploratory spatial analysis indicates an altitude-related isotopic gradient, with more negative isotope values in higher-elevation areas and less negative values in lower-lying areas along the Vardar River. Statistical analysis identifies air temperature as the meteorological parameter most consistently associated with isotopic variability, showing strong and statistically significant positive correlations at all three stations, with the strongest relationships observed in Skopje. Relative humidity exhibits a relatively strong negative relationship with isotope values, particularly in Tetovo and Skopje, while precipitation amount shows a moderate negative relationship, most pronounced in Tetovo. Wind speed demonstrates variable and generally weak relationships, whereas atmospheric pressure has the lowest explanatory power. Additionally, the analysis of d-excess indicates relationships with meteorological parameters that may reflect seasonal variations in atmospheric moisture conditions and evaporation-related processes. These findings highlight the existence of the combined influence of seasonal changes, elevation, and local meteorological conditions on precipitation isotope composition, contributing to a better understanding of environmental and hydrometeorological processes and providing a basis for future applications of stable isotopes in water resource research within the Vardar River basin.

Keywords: stable isotopes of water; precipitation; seasonal variation; Vardar River basin; isotopic composition; hydrological processes

Academic Editors: Wei Zhang and Maritza Arganis-Juarez

Received: 6 November 2026
Revised: 25 November 2026
Accepted: 26 November 2026
Published: 28 November 2026

Copyright: © 2026 by the authors. Licensee MDPI, Basel, Switzerland. This article is an open access article distributed under the terms and conditions of the Creative Commons Attribution (CC BY) license.

1. Introduction

Stable isotopes of oxygen ($\delta^{18}O$) and hydrogen ($\delta^{2}H$) are widely used in hydrological and climatological research to investigate water origin, atmospheric moisture transport, precipitation-forming processes, and the dynamics of the hydrological cycle [1–5]. Their composition reflects isotope fractionation during evaporation and condensation, as well as atmospheric circulation and moisture sources [6–8]. Stable isotope analysis also provides valuable insights into environmental processes by helping to identify the influence of climatic variability and changing environmental conditions on the hydrological cycle. The temporal and spatial variability of precipitation isotopes is controlled by several interacting factors, including air temperature, precipitation amount, relative humidity, altitude, continentality, and moisture transport pathways [2–4,9,10]. Although precipitation is generally enriched in heavier isotopes during warmer months and depleted during colder periods, the magnitude of these patterns varies depending on regional climatic and atmospheric conditions [4,9,10].

Recent studies have demonstrated that the influence of meteorological parameters on precipitation isotope composition differs considerably among geographical regions. Investigations in the Shiyang River basin, the northern Tibetan Plateau, and the Bay of Bengal have highlighted the combined effects of local moisture recycling, atmospheric circulation, moisture sources, and topographical conditions [11–13]. Similarly, research conducted in different climatic environments has shown that isotope–temperature relationships are not uniform and depend on regional atmospheric circulation and moisture transport processes [14,15]. These findings emphasize the importance of considering multiple meteorological and geographical factors when interpreting precipitation isotope variability and its environmental significance.

The relationship between $\delta^{2}H$ and $\delta^{18}O$ provides an additional basis for investigating precipitation characteristics. Craig [1] established the Global Meteoric Water Line (GMWL), while subsequent studies demonstrated that local and regional meteoric water lines may differ due to variations in moisture sources, humidity, evaporation, and precipitation-forming conditions [4,6,16]. Local meteoric water lines therefore provide valuable reference information for regional isotope investigations and subsequent hydrological studies [5,6,17]. Deuterium excess (d-excess), another parameter derived from the relationship between $\delta^{2}H$ and $\delta^{18}O$, provides complementary information on moisture source conditions and non-equilibrium fractionation processes [2]. Its spatial and temporal variability reflects the combined influence of relative humidity in moisture source regions, atmospheric transport, and below-cloud evaporation [18–20].

Systematic stable isotope monitoring represents an important basis for understanding precipitation isotope variability and its relationship with climatic and environmental conditions. The Global Network of Isotopes in Precipitation (GNIP) provides essential observational data for investigating spatial and seasonal isotope patterns and their relationships with climate and atmospheric circulation [21,22]. Studies in Southeast Europe have also demonstrated the importance of isotope observations for identifying regional precipitation characteristics and the influence of meteorological conditions and air mass origins [23,24]. Broader regional assessments, including the compilation of precipitation isotope data from 842 stations across Eurasia, have further contributed to understanding geographical and seasonal patterns [25].

The temporal resolution of isotope sampling is another important consideration. Monthly isotope values integrate several precipitation events and may therefore obscure short-term variations associated with rainfall intensity, condensation conditions, and changes in moisture sources [8,16]. Although daily and sub-daily observations provide more detailed information on these processes [26,27], monthly monitoring remains valuable for assessing broader seasonal patterns when combined with meteorological data.

https://doi.org/10.3390/environments13120659

Geographical characteristics, particularly elevation, continentality, and atmospheric moisture transport, also contribute to the spatial distribution of precipitation isotopes [7]. Spatial modelling can support the interpretation of these patterns [28]; however, the reliability of such estimates depends on the number, distribution, and representativeness of monitoring stations, particularly in regions with complex topography and limited observational data. The Vardar River basin in North Macedonia provides an interesting setting for investigating precipitation isotope variability because of its considerable elevation differences and the combined influence of continental and Mediterranean climatic conditions. These characteristics may affect precipitation isotope composition through variations in atmospheric moisture sources, transport pathways, and local meteorological conditions. Research on stable isotopes in precipitation, surface waters, and groundwater within the Vardar River basin remains relatively limited. A recent investigation [29] provided an initial isotope-hydrological characterization of these water components, showing that surface water and groundwater generally exhibited more depleted isotopic compositions than precipitation, suggesting contributions from higher-elevation and/or colder-season recharge. Similar isotopic signatures at selected surface water and groundwater locations also indicated potential hydrological connections. However, a more detailed assessment of precipitation isotope variability, its relationships with meteorological parameters, and its seasonal and spatial characteristics remains necessary.

Therefore, this study aims to investigate the seasonal and spatial variability of stable oxygen and hydrogen isotopes ($\delta^{18}O$ and $\delta^{2}H$) in precipitation within the Vardar River basin, based on observations collected at three monitoring stations between June 2025 and June 2026. The specific objectives are to characterize temporal isotope variations, assess spatial differences among monitoring stations in relation to their geographical and elevation characteristics, and examine relationships between isotope composition and meteorological parameters, including air temperature, precipitation amount, relative humidity, wind speed, and atmospheric pressure. The study also examines seasonal variations in d-excess, establishes local and regional meteoric water lines, and evaluates spatial isotope distributions using distance-based interpolation and elevation-dependent regression.

The originality of this study lies in its integrated assessment of seasonal and spatial precipitation isotope variability, meteorological relationships, and geographical influences within an environmental and hydrological context. By extending and complementing previous preliminary investigations [29] with additional monitoring data and a broader analytical approach, including detailed seasonal analysis, statistical evaluation of isotope–meteorological relationships, and complementary spatial modelling methods, this research contributes to a more comprehensive understanding of precipitation isotope dynamics and their environmental significance. The results provide valuable reference information for future environmental and isotope hydrological investigations, supporting the assessment of water resources, groundwater recharge processes, surface water–groundwater interactions, and sustainable water resource management in North Macedonia and the wider Balkan region.

2. Study Area

The study area consists of the portion of the Vardar River basin located within the territory of the Republic of North Macedonia (Figure 1). The research area covers 20,444 km^2 (79.5% of the territory of the Republic of North Macedonia). The Vardar is the principal and longest river within it, with a total length of 388 km to the Aegean Sea (301 km of which lie within Macedonia) [30]. The basin is characterized by diverse topography. The highest point in the basin is the 2764 m a.s.l.-high Korab Peak on the mountain of the same name, while the lowest point is in Gevgelija (46 m a.s.l.), where the river leaves Macedonia and continues into Greece, eventually flowing into the Aegean Sea.

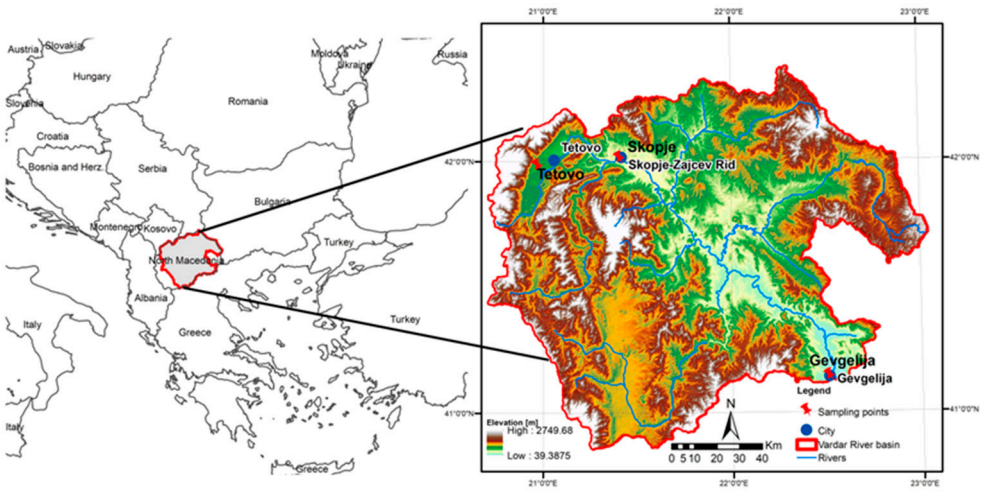

Figure 1. Map showing the location of the Vardar River basin and the sampling points.

The diversity of climatic conditions within the basin is primarily determined by the varied terrain and geographical location. The northern part of the Vardar River basin features a temperate continental climate, while the southern areas are influenced by the Mediterranean climate [31]. The uneven distribution of precipitation across the basin is influenced by both topography and seasonality. Average annual precipitation ranges from 500 to 800 mm. In mountainous regions, this figure exceeds 1000 mm, whereas in the central part, it falls below the average. Precipitation is highest during the spring and autumn months, often falling as snow in the higher elevations. The summer months are relatively dry, particularly in the central part of the basin—such as the area around Skopje—where months without precipitation have been recorded [32]. Seasonal air temperature variation within the basin is particularly pronounced. The average annual temperature ranges from 10 °C to 13 °C; however, temperatures frequently drop below 0 °C during the winter months, while summers are warm to hot, with temperatures potentially reaching up to 40 °C, especially in the Vardar Valley [33].

3. Data and Methodology

3.1. Precipitation Sampling and Isotopes

Precipitation samples were collected at monthly intervals from three monitoring stations: Tetovo (Latitude 41° 59′ 09.55″ N, longitude: 20° 57′ 53.98″ E and elevation at 451.23 m a.s.l.), Skopje (Latitude 42° 00′ 59.81″ N, longitude: 21° 24′ 00.15″ E and elevation at 301.02 m a.s.l.) and Gevgelija (Latitude 41° 08′ 48.52″ N, longitude: 22° 30′ 11.04″ E and elevation at 57.49 m a.s.l.), Figure 1. Between June 2025 and June 2026, a total of 38 precipitation samples were collected from three different stations. However, 37 samples were included in the final analysis (13 from Tetovo, 13 from Skopje, and 11 from Gevgelija). No sample was collected in Gevgelija in June 2025 due to the absence of precipitation, while the October 2025 sample from this station was excluded from the analysis due to suspected evaporation. The samples were collected using PALMEX RS-1-type precipitation collectors (Palmex d.o.o, Zagreb, Croatia), which consist of a funnel with a 13.5 cm diameter and a 3-litre HDPE collection vessel. Palmex RS-1 collectors have been shown to protect water samples from evaporation and are suitable for use in most hydrological studies [34,35]. Each month, the collected water samples were transferred into 50 mL HDPE bottles and stored in a refrigerator at a temperature of 4 °C.

The stable isotope composition of the water samples was analyzed with a Liquid Water Isotope Analyzer (LWIA-45-EP, Los Gatos Research, ABB, San Jose, CA, USA) in the

Laboratory for Spectroscopy of the Faculty of Mining, Geology and Petroleum Engineering, University of Zagreb, Croatia. Each sample was analyzed in two independent runs, with a total of nine injections (4 + 5) in each run. The official Los Gatos Research (LGR) working standards were used for normalization purposes. The results are presented in ‰ notation relative to VSMOW (Vienna Standard Mean Ocean Water) with an analytical uncertainty of ±0.19‰ for $\delta^{18}O$ and ±0.9‰ for $\delta^{2}H$. Data processing and interpretation were performed by the Laboratory Information Management System (LIMS) for lasers [36].

3.2. Meteorological Data

The meteorological data used in this study were obtained from different sources, depending on the parameter considered. Precipitation amounts were measured directly at the monitoring sites during each water-sampling campaign for stable isotope analysis. Air temperature and wind speed data were obtained from the Meteostat database (https://meteostat.net; accessed on 15 October 2026), while relative humidity and atmospheric pressure data were retrieved from the Copernicus Climate Change Service (C3S) Climate Data Store (DOI: 10.24381/cds.adbb2d47; accessed on 15 October 2026). These datasets were used to investigate the relationships between the isotopic composition of precipitation and the corresponding meteorological conditions at the three monitoring stations.

3.3. Methodology

The isotopic composition of precipitation was investigated through a comprehensive analysis of its seasonal and spatial variability, as well as the influence of meteorological parameters and altitude to better understand the relationships between precipitation isotopes and regional environmental conditions. Seasonal variability was examined to identify temporal changes in $\delta^{18}O$ and $\delta^{2}H$ values throughout the study period, while spatial variability was assessed to characterize differences in isotopic composition among monitoring stations—both by season (spring: March–April–May; summer: June–July–August; autumn: September–October–November; winter: December–January–February) and by the winter (October–April) and summer (May–September) half-year periods. The deuterium excess (d-excess) was calculated using the slope of the Global Meteoric Water Line (GMWL) established by Araguás-Araguás et al. [37]. Accordingly, d-excess was calculated as d-excess = $\delta^{2}H - 7.96 \cdot \delta^{18}O$. The relationships between precipitation isotopes and meteorological parameters, including air temperature, precipitation amount, relative humidity, wind speed and atmospheric pressure, were analyzed using regression analysis to evaluate their associations with isotopic variability under different environmental and climatic conditions. Additionally, Pearson's correlation coefficient (r) was calculated to quantify the strength and direction of the linear relationships between $\delta^{18}O$, $\delta^{2}H$, d-excess, and the meteorological parameters at each monitoring station. The statistical significance of the correlations was evaluated using two-tailed tests, with significance levels of $p \leq 0.05$ and $p \leq 0.01$. Correlations were calculated separately for each station using the available valid monthly observations (n = 13 for Tetovo and Skopje; n = 11 for Gevgelija). Local Meteoric Water Lines (LMWLs) and a Regional Meteoric Water Line (RMWL) were established; by comparing these with each other and with the Global Meteoric Water Line (GMWL), regional differences in the characteristics of meteoric waters were assessed. The effect of altitude was investigated to assess the relationship between elevation and isotopic composition, which provided further insight into the spatial distribution of isotopes in precipitation across the study area. The spatial distribution of stable isotopes in precipitation was analyzed using two approaches: Inverse Distance Weighting (IDW) interpolation and an elevation-based regression model. The IDW method estimates isotopic values at unsampled locations based on distance-weighted observations from surrounding mon-

itoring stations, assigning greater influence on nearby stations without explicitly accounting for spatial autocorrelation [38]. This method was selected due to its simplicity and applicability to datasets with a limited number of monitoring stations, providing a straightforward representation of spatial isotope variability based on the available observations. The second approach was based on the relationship between elevation and precipitation isotopic composition, which has been widely applied in spatial isotope modelling [7,39]. A linear regression equation relating isotopic composition to elevation was established using the observed precipitation isotope values and the elevations of the monitoring stations (Table A4). The resulting regression equation was applied directly to a Digital Elevation Model (DEM) using raster-based mathematical operations in ArcGIS Desktop 10.5 (Esri, Redlands, CA, USA), allowing isotopic values to be estimated for each raster cell according to its elevation. This approach follows the principles of elevation-dependent isotope mapping [7,39] and enables the representation of potential topographically controlled spatial variations in precipitation isotopes across the Vardar River basin. Together, these approaches provide complementary perspectives on spatial isotope variability and help assess the sensitivity of estimated isotope distributions to different modelling assumptions. However, given the limited number of monitoring stations, the spatial analysis is considered exploratory, and the resulting maps should be interpreted as indicative rather than validated basin-wide isotope distributions. A denser monitoring network would be required to improve the reliability of spatial estimates and their application in environmental and hydrological assessments.

4. Results and Discussion

4.1. Seasonal Variability of Precipitation Isotopes

Monthly values for stable isotopes in precipitation and d-excess for the three monitoring stations are presented in Appendix A. Graphical representations of the temporal distribution of stable isotopes and d-excess in Tetovo, Skopje, and Gevgelija are shown in Figure 2, respectively. Table 1 shows the mean values of stable isotope content and d-excess categorized by season—spring (March–April–May), summer (June–July–August), autumn (September–October–November), and winter (December–January–February)—as well as by the winter half-year (October–April) and the summer half-year (May–September). Table 2 presents the descriptive statistical analysis of precipitation isotope data and d-excess in Tetovo, Skopje and Gevgelija.

The results demonstrate a pronounced seasonal pattern at all three stations, characterized by isotopic enrichment during summer and depletion during winter. At the Tetovo monitoring station, the average values were −7.05‰ for $\delta^{18}O$ and −46.4‰ for $\delta^{2}H$. The most depleted values were recorded in January 2026 ($\delta^{18}O$ = −11.53 ‰, $\delta^{2}H$ = −79.6‰), while the most enriched values occurred in June 2026 ($\delta^{18}O$ = −2.21‰, $\delta^{2}H$ = −18.2 ‰). The d-excess values ranged from −0.6‰ to 17.9‰, with an average of 9.67‰. Regarding the seasons, the data show that summer precipitation in Tetovo is the most isotopically enriched ($\delta^{18}O$ = −3.79‰, $\delta^{2}H$ = −25.5‰, d-excess = 4.7‰), while winter precipitation is the most depleted ($\delta^{18}O$ = −10.73‰, $\delta^{2}H$ = −71.9‰, d-excess = 13.5‰). The sample with ID 2 from the Skopje monitoring station, Table A2, corresponding to July 2025 (collection date: 1 August 2025), shows a slightly negative d-excess value (−0.8‰), suggesting possible sample evaporation; however, an examination of the stable isotope values reveals no deviation from the other data, so it was decided to include the results for this sample in the analysis. Analysis of precipitation samples collected at the Skopje monitoring station showed that the average $\delta^{18}O$ value in precipitation was −6.90‰, while the average $\delta^{2}H$ value was −46.1‰. The most depleted values were observed in January 2026 ($\delta^{18}O$ = −11.65‰, $\delta^{2}H$ = −83.7‰), whereas the most enriched values were recorded in June 2026 for $\delta^{18}O$ (−2.77‰) and September 2025 for $\delta^{2}H$ (−19.5‰). The d-excess values ranged from

−0.8 ‰ to 16.4‰, with an average of 8.8‰. Regarding the seasons, the data show that summer precipitation in Skopje is isotopically enriched ($\delta^{18}O$ = −3.85 ‰, $\delta^{2}H$ = −27.2 ‰, d-excess = 3.4 ‰), whereas winter precipitation is isotopically depleted ($\delta^{18}O$ = −10.50 ‰, $\delta^{2}H$ = −71.6 ‰, d-excess = 12.0 ‰). The sample with ID5 from the monitoring station in Gevgelija (Table A3), corresponding to October 2025, shows a very negative value for "d-excess" (d-excess = −14.7‰), indicating evaporation of the sample; furthermore, the analysis of stable isotope values revealed a deviation compared to the other data, and it was therefore decided to exclude the results for this sample from the analysis. No precipitation was recorded in Gevgelija for June 2025; consequently, there is no sample to analyze. Analysis of the precipitation samples collected at the monitoring station in Gevgelija (11 in total) showed an average $\delta^{18}O$ value of −6.11‰, while the average $\delta^{2}H$ value was −38.4‰. The most depleted values were observed in January 2026 ($\delta^{18}O$ = −9.77‰, $\delta^{2}H$ = −66.3‰), whereas the most enriched values were recorded in June 2026 for $\delta^{18}O$ (−2.28‰) and September 2025 for $\delta^{2}H$ (−12.4‰). The "d-excess" values ranged from 0.3‰ to 17.1‰, with an average of 10.2‰. Seasonal data show that summer precipitation in Gevgelija is isotopically enriched ($\delta^{18}O$ = −4.23‰, $\delta^{2}H$ = −28.7‰, d-excess = 5.0‰), while winter precipitation is isotopically depleted ($\delta^{18}O$ = −9.37‰, $\delta^{2}H$ = −60.8‰, d-excess = 13.9‰).

Table 1. Isotopic composition (average values for $\delta^{2}H$ and $\delta^{18}O$) of precipitation and d-excess by season.

Seasons	Month	$\delta^{2}H$, in ‰	$\delta^{18}O$, in ‰	d-excess
Tetovo				
summer	JJA	−25.5	−3.79	4.7
autumn	SON	−52.4	−8.30	13.6
winter	DJF	−71.9	−10.73	13.5
spring	MAM	−43.1	−6.47	8.5
winter half-year	(Oct–Apr)	−64.6	−9.72	12.8
summer half-year	(May–Sep)	−25.3	−3.94	6.1
Skopje				
summer	JJA	−27.2	−3.85	3.4
autumn	SON	−50.4	−8.02	13.4
winter	DJF	−71.6	−10.50	12.0
spring	MAM	−41.6	−6.25	8.2
winter half-year	(Oct-Apr)	−64.1	−9.61	12.3
summer half-year	(May–Sep)	−25.8	−3.91	5.3
Gevgelija				
summer	JJA	−28.7	−4.23	5.0
autumn	SON	−27.7	−5.32	14.7
winter	DJF	−60.8	−9.37	13.9
spring	MAM	−33.1	−5.26	8.8
winter half-year	(Oct–Apr)	−51.0	−8.04	13.0
summer half-year	(May–Sep)	−23.4	−3.80	6.9

The consistent winter depletion and summer enrichment across all three stations indicate a strong seasonal influence on precipitation isotope composition, in agreement with previous studies [40–42]. These variations are consistent with seasonal changes in atmospheric temperature, precipitation characteristics, and moisture-related processes. The generally higher winter d-excess values and lower summer values further suggest seasonal differences in moisture conditions and potential evaporation effects, demonstrating how precipitation isotopes can serve as indicators of seasonal environmental conditions and atmospheric processes in the Vardar River basin.

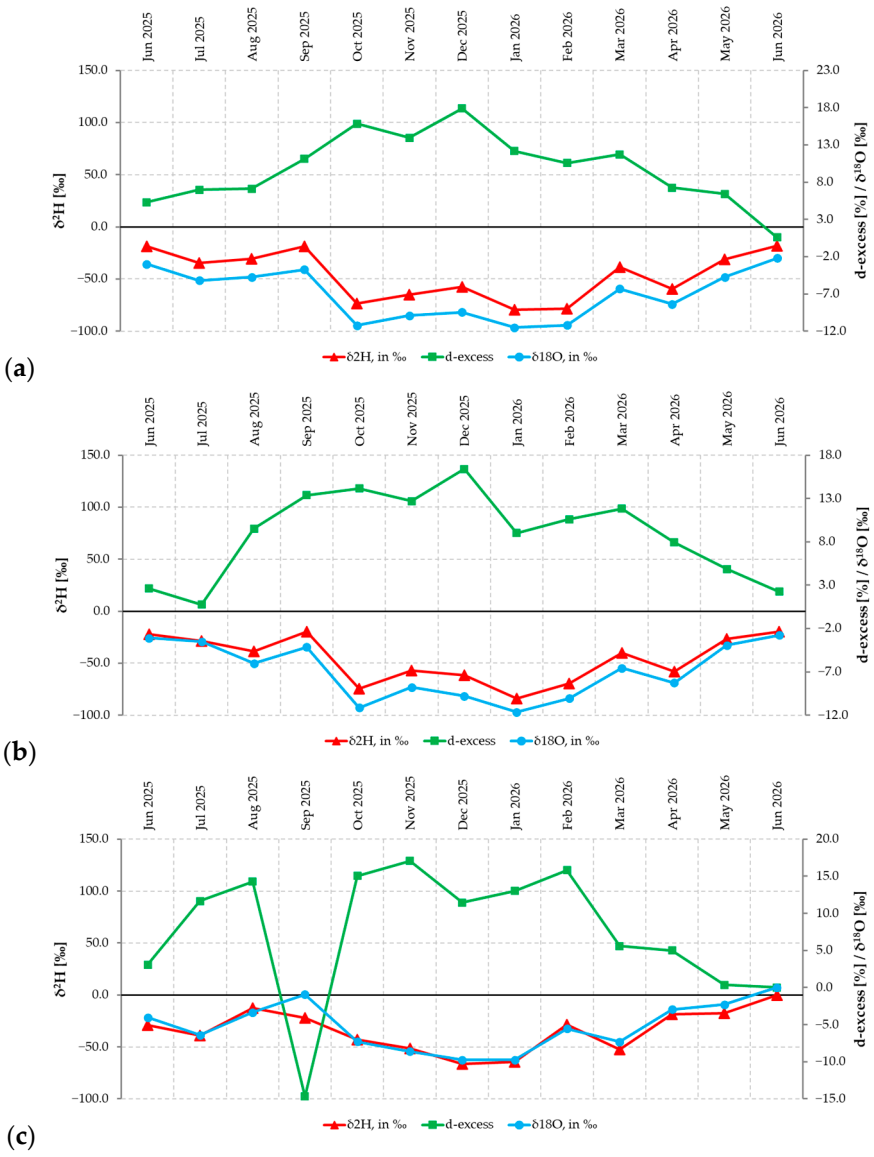

Figure 2. Temporal distribution of stable isotopes and d-excess in (**a**) Tetovo, (**b**) Skopje, and (**c**) Gevgelija.

The descriptive statistical analysis of stable isotopes in precipitation reveals differences in isotopic composition and variability among the three monitoring stations. The highest standard deviations are observed in Tetovo, reaching 3.37‰ for $\delta^{18}O$ and 23.4‰ for $\delta^{2}H$, followed by Skopje with corresponding values of 3.22‰ and 22.4‰. In contrast, Gevgelija exhibits the lowest variability, with standard deviations of 2.70‰ for $\delta^{18}O$ and 18.8‰ for $\delta^{2}H$. Regarding d-excess, the highest mean value is observed in Gevgelija (10.2‰), followed by Tetovo (9.7‰) and Skopje (8.8‰), indicating relatively small differences in average d-excess among the monitoring stations. Unlike $\delta^{18}O$ and $\delta^{2}H$, d-excess exhibits the greatest variability in Gevgelija, with a standard deviation of 5.7‰, followed by Skopje (5.2‰) and Tetovo (4.9‰). However, Tetovo shows the widest range of d-excess values (18.5‰), compared with Skopje (17.2‰) and Gevgelija (16.7‰). The relatively greater variability of $\delta^{18}O$ and $\delta^{2}H$ in Tetovo and Skopje may reflect stronger temporal changes in meteorological conditions and precipitation characteristics, whereas the lower variability in Gevgelija suggests a comparatively narrower range of isotopic conditions during the observation period. The contrasting variability of d-excess suggests that the processes influencing this parameter may differ from those governing the isotopic composition of $\delta^{18}O$ and $\delta^{2}H$. The distributions of both isotopes exhibit skewness values close

to zero, indicating approximately symmetric distributions at all three stations. In contrast, d-excess exhibits slightly negative skewness at all stations, particularly in Gevgelija (−0.6), suggesting a somewhat greater tendency toward lower values. Furthermore, the consistently negative kurtosis values for $\delta^{18}O$ and $\delta^{2}H$ indicate relatively flat distributions compared with the normal distribution, while d-excess exhibits mixed kurtosis values, ranging from 0.3 in Tetovo to −1.2 in Gevgelija, indicating differences in distribution shape among the stations. Overall, the descriptive statistics demonstrate that precipitation in Gevgelija is relatively enriched in heavy isotopes and exhibits lower temporal variability in $\delta^{18}O$ and $\delta^{2}H$, but slightly higher mean d-excess and greater d-excess variability, whereas Tetovo and Skopje are characterized by more depleted mean isotopic compositions and greater fluctuations in $\delta^{18}O$ and $\delta^{2}H$ during the investigated period.

Table 2. Descriptive statistical analysis of data on isotope content in precipitation.

	Tetovo			**Skopje**			**Gevgelija**		
	$\delta^{2}H$, in ‰	**$\delta^{18}O$, in ‰**	**d-excess in ‰**	**$\delta^{2}H$, in ‰**	**$\delta^{18}O$, in ‰**	**d-excess in ‰**	**$\delta^{2}H$, in ‰**	**$\delta^{18}O$, in ‰**	**d-excess in ‰**
Mean	−46.4	−7.05	9.7	−46.1	−6.90	8.8	−38.4	−6.11	10.2
Standard Error	6.5	0.94	1.4	6.2	0.89	1.4	5.7	0.81	1.7
Median	−38.6	−6.32	10.6	−40.3	−6.55	9.5	−39.2	−6.39	11.7
Standard Deviation	23.4	3.37	4.9	22.4	3.22	5.2	18.8	2.70	5.7
Kurtosis	−1.6	−1.65	0.3	−1.4	−1.64	−0.7	−1.3	−1.43	−1.2
Skewness	−0.2	−0.07	−0.3	−0.3	−0.10	−0.5	−0.2	0.02	−0.6
Range	61.4	9.32	18.5	64.2	8.88	17.2	53.9	7.49	16.7
Minimum	−79.6	−11.53	−0.6	−83.7	−11.65	−0.8	−66.3	−9.77	0.3
Maximum	−18.2	−2.21	17.9	−19.5	−2.77	16.4	−12.4	−2.28	17.1
Count	13	13	13	13	13	13	11	11	11

4.2. Spatial Variability of Precipitation Isotopes

The spatial variability of stable isotopes in precipitation across the Vardar River basin was examined on a seasonal basis—summer (JJA), autumn (SON), winter (DJF), and spring (MAM)—as well as for two distinct periods: the summer half-year (May–September) and the winter half-year (October–April), using exploratory spatial modelling approaches (Figures A1 and A2, Appendix A).

In autumn, winter, and spring, estimated spatial patterns generally suggested more depleted values in the northwestern and higher-elevation areas and enriched values towards the southeastern, lower-lying part of the basin. This altitudinal gradient was also evident in the half-year distributions, suggesting a general decrease in $\delta^{2}H$ and $\delta^{18}O$ values with increasing elevation, as shown in Figures A1 and A2.

The d-excess exhibited pronounced seasonal variability, with the highest values during autumn (13.4‰ in Skopje–14.7‰ in Gevgelija) and winter (12.0‰ in Skopje–13.9‰ in Gevgelija), consistent with observations at Murska Sobota during 2016–2024 [17]. Lower values occurred in spring (8.2–8.8‰), while summer showed the lowest values (3.4–5.0‰). The IDW maps (Figure A1) suggest relatively uniform d-excess during autumn, whereas the other seasons show lower values around Skopje and higher values towards the northwestern and southeastern parts of the basin. A similar contrast was observed between the summer and winter half-years, with d-excess ranging from 5.3‰ in Skopje to 6.9‰ in Gevgelija and from 12.3‰ to 13.0‰, respectively. These seasonal differences may reflect variations in atmospheric moisture conditions and evaporation processes, although the limited spatial coverage prevents a definitive interpretation of their geographical distribution.

The estimated vertical isotopic gradients exhibited considerable seasonal variability across the Vardar River basin (Table A4). During the summer half-year (May–September), relatively weak negative gradients were obtained for $\delta^{18}O$ (−0.04‰/100 m) and $\delta^{2}H$ (−0.5‰/100 m), whereas substantially steeper gradients occurred during the winter half-year (October–April), reaching −0.44‰/100 m and −3.6‰/100 m, respectively. Seasonally, the strongest negative gradients were observed in autumn (SON), with −0.79‰/100 m for $\delta^{18}O$ and −6.6‰/100 m for $\delta^{2}H$, followed by winter (DJF; −0.36 and −3.0‰/100 m) and spring (MAM; −0.32 and −2.6‰/100 m). In contrast, summer (JJA) exhibited positive gradients, indicating a reversed altitude effect, potentially influenced by differences in monthly sampling coverage, particularly the absence of precipitation in Gevgelija in June 2025. The annual gradients were −0.25‰/100 m for $\delta^{18}O$ and −2.1‰/100 m for $\delta^{2}H$, comparable to the −0.22‰/100 m $\delta^{18}O$ gradient reported by Giustini et al. [43] across Italy. However, these gradients are based on only three monitoring stations and should be regarded as preliminary estimates rather than established basin-wide altitude effects.

Unlike $\delta^{18}O$ and $\delta^{2}H$, d-excess exhibited negative vertical gradients throughout the year, ranging from −0.10‰/100 m in spring to −0.28‰/100 m in autumn. The strongest relationship occurred during autumn (R^2 = 0.7107), compared with considerably weaker relationships in summer (R^2 = 0.1042) and winter (R^2 = 0.0840). The gradients were −0.25‰/100 m and −0.1‰/100 m during the summer and winter half-years, respectively, while the annual gradient was −0.18‰/100 m (R^2 = 0.2515). Although d-excess generally tends to increase slightly with elevation, with reported gradients of 0.1–0.5‰/100 m in humid regions [44], negative relationships have also been observed in arid areas of northwest China [45]. The seasonal differences may reflect variations in moisture sources, relative humidity and evaporation processes, particularly enhanced below-cloud evaporation during summer. Nevertheless, the generally weak elevation relationships suggest that altitude is not a dominant predictor of d-excess variability within the available observations.

The elevation-based model also generated a wider range of predicted isotope values, especially at higher elevations, as shown in Figure A2. Similar differences were observed for d-excess, with generally lower predicted values in mountainous areas. For example, during autumn (SON), d-excess ranged from 13.4‰ to 14.7‰ in the IDW model, compared with 8.6–14.9‰ in the elevation-based model; during summer (JJA), the corresponding ranges were 3.4–5.0‰ and 0.9–4.7‰. However, the relatively weak d-excess–elevation relationships, together with extrapolation beyond the elevation range of the three monitoring stations, introduce uncertainty into the elevation-based predictions. This limitation is particularly important because the three monitoring stations do not fully represent the basin's elevation range, meaning that predictions for higher mountainous areas involve extrapolation and should therefore be interpreted with caution. Although the elevation-based approach provides greater representation of topographic influences, both methods should be considered complementary. Similar methodological differences between distance-based and elevation-informed spatial modelling have been reported by Schneck et al. [46] and Mair and Fares [47], while Bowen and Revenaugh [39] emphasized the importance of geographical and elevation-related effects in precipitation isotope interpolation.

Overall, the spatial modelling results provide an exploratory perspective on how geographical characteristics and environmental conditions may be associated with precipitation isotope variability across the Vardar River basin. However, because both modelling approaches rely on observations from only three monitoring stations, additional monitoring stations would be necessary to improve their reliability and support more detailed environmental and hydrological assessments.

4.3. Effect of Meteorological Parameters on the Isotopic Composition of Precipitation

The relationship between precipitation stable isotopes ($\delta^{18}O$ and $\delta^{2}H$) and meteorological parameters at Tetovo, Skopje, and Gevgelija was analyzed using linear regression equations and the coefficient of determination (R^2). The relationships are presented in Appendix B (Figures A3–A5), while the corresponding regression equations and R^2 values for precipitation amount (P), air temperature (T), wind speed (W), atmospheric pressure (Ap), and relative humidity (RH) are summarized in Table 3. Additionally, Pearson's correlation coefficients (r) and their corresponding *p*-values are presented in Table 4, providing information on the direction, strength, and statistical significance of the relationships between meteorological parameters, stable isotopes, and d-excess. Figure 3 illustrates the temporal variations in meteorological parameters and isotope composition at the three stations.

Among the investigated parameters, air temperature showed the strongest and most consistent positive relationship with both isotopes. For $\delta^{18}O$, the coefficients of determination were $R^2 = 0.723$ in Tetovo, 0.7649 in Skopje, and 0.621 in Gevgelija, while the corresponding values for $\delta^{2}H$ were 0.6892, 0.7087, and 0.5039, respectively (Table 3). Pearson correlation analysis (Table 4) confirmed strong and statistically significant positive correlations between temperature and $\delta^{18}O$ in Tetovo ($r = 0.850$, $p < 0.001$), Skopje ($r = 0.875$, $p < 0.001$), and Gevgelija ($r = 0.788$, $p = 0.004$). Similar significant positive correlations were observed for $\delta^{2}H$, with $r = 0.830$ ($p < 0.001$), 0.842 ($p < 0.001$), and 0.710 ($p = 0.014$), respectively. Thus, the strongest temperature–isotope relationships were observed in Skopje, followed by Tetovo and Gevgelija. The sensitivity of isotope composition to temperature also varied seasonally. The $\delta^{18}O$ changes per 1 °C were 0.43‰ in Tetovo (0.62‰ in winter and 0.33‰ in summer), 0.35‰ in Skopje (0.46‰ and 0.32‰), and 0.32‰ in Gevgelija (0.50‰ and 0.41‰), respectively. For $\delta^{2}H$, the corresponding annual changes were 2.8‰/°C in Tetovo, 2.6‰/°C in Skopje, and 2.3‰/°C in Gevgelija. These values increased during winter to 4.9, 3.9, and 4.5‰/°C, respectively, while during summer they were 1.8, 1.9, and 2.7‰/°C. Overall, the stronger temperature-related isotope changes during winter indicate greater seasonal sensitivity compared with summer, consistent with the findings of Field et al. [48], who reported stronger winter temperature–$\delta^{18}O$ correlations across Europe. These results highlight the close association between seasonal temperature variability and precipitation isotope composition under the environmental and climatic conditions of the Vardar River basin. The relationship between d-excess and temperature showed a consistent negative trend at all three monitoring stations, with regression slopes ranging from −0.4451 to −0.4022. The strongest relationship was observed at Tetovo ($R^2 = 0.4783$), followed by Skopje ($R^2 = 0.4715$), while Gevgelija showed a weaker relationship ($R^2 = 0.3864$). Pearson correlation coefficients (Table 4) also indicated statistically significant negative relationships between temperature and d-excess in Tetovo ($r = -0.692$, $p = 0.009$), Skopje ($r = -0.687$, $p = 0.010$), and Gevgelija ($r = -0.622$, $p = 0.041$). The higher R^2 values compared with those for d-excess and precipitation amount ($R^2 = 0.1490$–0.2212) indicate that temperature explains a greater proportion of d-excess variability during the study period. However, these relationships may also reflect seasonal variations in atmospheric circulation, moisture source regions, and humidity conditions during evaporation, as discussed by Pfahl and Sodemann [18] and Türk et al. [27].

Table 3. Relationship between stable isotope content in precipitation and meteorological parameters.

	$\delta^{18}O$	$\delta^{2}H$	d-excess
		Tetovo	
P	$\delta^{18}O = -0.038 \times P - 4.4251$ ($R^2 = 0.5541$)	$\delta^{2}H = -0.2709 \times P - 27.938$ ($R^2 = 0.5733$)	d-excess = $0.0349 \times P + 7.2865$ ($R^2 = 0.2132$)
T	$\delta^{18}O = 0.3735 \times T - 12.264$ ($R^2 = 0.723$)	$\delta^{2}H = 2.5278 \times T - 81.617$ ($R^2 = 0.6892$)	d-excess = $-0.4451 \times T + 15.864$ ($R^2 = 0.4783$)
W	$\delta^{18}O = -0.4017 \times W - 4.8677$ ($R^2 = 0.0047$)	$\delta^{2}H = -6.1583 \times W - 12.989$ ($R^2 = 0.0231$)	d-excess = $-2.9608 \times W + 25.757$ ($R^2 = 0.1194$)
Ap	$\delta^{18}O = 0.1713 \times Ap - 181.07$ ($R^2 = 0.0183$)	$\delta^{2}H = 1.9041 \times Ap - 1981.1$ ($R^2 = 0.047$)	d-excess = $0.5408 \times Ap - 539.8$ ($R^2 = 0.0849$)
RH	$\delta^{18}O = -0.2132 \times RH + 7.854$ ($R^2 = 0.7142$)	$\delta^{2}H = -1.4415 \times RH + 54.32$ ($R^2 = 0.6793$)	d-excess = $0.2556 \times RH - 8.1981$ ($R^2 = 0.4783$)
		Skopje	
P	$\delta^{18}O = -0.0575 \times P - 4.2739$ ($R^2 = 0.4375$)	$\delta^{2}H = -0.4034 \times P - 27.686$ ($R^2 = 0.4457$)	d-excess = $0.0542 \times P + 6.334$ ($R^2 = 0.149$)
T	$\delta^{18}O = 0.3173 \times T - 11.748$ ($R^2 = 0.7649$)	$\delta^{2}H = 2.1232 \times T - 78.562$ ($R^2 = 0.7087$)	d-excess = $-0.4022 \times T + 14.955$ ($R^2 = 0.4715$)
W	$\delta^{18}O = 1.3624 \times W - 16.832$ ($R^2 = 0.2319$)	$\delta^{2}H = 7.6228 \times W - 101.69$ ($R^2 = 0.1502$)	d-excess = $-3.2219 \times W + 32.297$ ($R^2 = 0.4975$)
Ap	$\delta^{18}O = -0.218 \times Ap - 214.59$ ($R^2 = 0.0352$)	$\delta^{2}H = -0.5795 \times Ap + 542.62$ ($R^2 = 0.0051$)	d-excess = $1.1559 \times Ap - 1165.5$ ($R^2 = 0.3798$)
RH	$\delta^{18}O = -0.2119 \times RH + 7.5816$ ($R^2 = 0.6814$)	$\delta^{2}H = -1.418 \times RH + 50.815$ ($R^2 = 0.6316$)	d-excess = $0.2683 \times RH - 9.5345$ ($R^2 = 0.4194$)
		Gevgelija	
P	$\delta^{18}O = -0.0267 \times P - 4.2227$ ($R^2 = 0.4323$)	$\delta^{2}H = -0.1723 \times P - 26.26$ ($R^2 = 0.3684$)	d-excess = $0.0405 \times P + 7.3525$ ($R^2 = 0.2212$)
T	$\delta^{18}O = 0.2524 \times T - 10.112$ ($R^2 = 0.621$)	$\delta^{2}H = 1.5877 \times T - 63.593$ ($R^2 = 0.5039$)	d-excess = $-0.42164 \times T + 16.894$ ($R^2 = 0.3864$)
W	$\delta^{18}O = -0.674 \times W + 0.6066$ ($R^2 = 0.1529$)	$\delta^{2}H = -4.9752 \times W + 10.832$ ($R^2 = 0.1686$)	d-excess = $0.4251 \times W + 6.0036$ ($R^2 = 0.0134$)
Ap	$\delta^{18}O = -0.0471 \times Ap + 41.709$ ($R^2 = 0.0022$)	$\delta^{2}H = 0.7504 \times Ap - 800.19$ ($R^2 = 0.0115$)	d-excess = $1.1254 \times Ap - 1132.2$ ($R^2 = 0.2818$)
RH	$\delta^{18}O = -0.1955 \times RH + 7.7342$ ($R^2 = 0.4832$)	$\delta^{2}H = -1.225 \times RH + 48.144$ ($R^2 = 0.3875$)	d-excess = $0.3337 \times RH - 13.42$ ($R^2 = 0.314$)

Precipitation amount showed a negative relationship with both isotopes at all three stations, indicating that higher precipitation amounts are generally associated with more depleted isotopic values. Similar findings were reported in central Croatia, where a moderate negative relationship between precipitation amount and $\delta^{18}O$ was observed during the warmer part of the year [49]. The strongest relationships were found in Tetovo ($\delta^{18}O$: $R^2 = 0.5541$; $\delta^{2}H$: $R^2 = 0.5733$), followed by Skopje ($R^2 = 0.4794$ and 0.4740, respectively), while Gevgelija showed weaker relationships ($R^2 = 0.4375$ and 0.4457), Table 3. Pearson correlation analysis (Table 4) confirmed statistically significant negative correlations between precipitation amount and $\delta^{18}O$ in Tetovo ($r = -0.744$, $p = 0.004$), Skopje ($r = -0.661$, $p = 0.014$), and Gevgelija ($r = -0.658$, $p = 0.028$). Similar negative correlations were observed for $\delta^{2}H$, with $r = -0.757$ ($p = 0.003$), -0.668 ($p = 0.013$), and -0.607 ($p = 0.048$), respectively. The estimated isotopic changes per 10 mm of precipitation were 0.49‰ for $\delta^{18}O$ and 3.2‰ for $\delta^{2}H$ in Tetovo, 0.76‰ and 5.5‰ in Skopje, and 0.34‰ and 2.5‰ in Gevgelija, respectively. Seasonally, the corresponding changes were 0.30‰ and 2.3‰ in winter and 0.70‰

and 3.8‰ in summer for Tetovo; 0.47‰ and 4.0‰ in winter and 0.73‰ and 4.3‰ in summer for Skopje; and 0.21‰ and 1.9‰ in winter and 0.62‰ and 4.1‰ in summer for Gevgelija. These patterns are consistent with the precipitation amount effect and related isotopic fractionation processes. The differences in seasonal sensitivity may also reflect variations in precipitation characteristics and local environmental conditions among the monitoring stations. In contrast, d-excess showed a positive relationship with precipitation amount at all three stations. The steepest regression slope occurred in Skopje (0.0542), followed by Gevgelija (0.0405) and Tetovo (0.0349). However, the relatively low and similar R^2 values (0.1490–0.2212) indicate that precipitation amount alone explains only a limited proportion of d-excess variability. Pearson correlation coefficients (Table 4) indicated positive but statistically non-significant correlations between precipitation amount and d-excess in Tetovo (r = 0.462, p = 0.112), Skopje (r = 0.386, p = 0.193), and Gevgelija (r = 0.470, p = 0.144). Other factors, including moisture-source characteristics, atmospheric circulation, and evaporation conditions during moisture transport, are also likely to contribute. Precipitation recycling may further influence d-excess, particularly in tropical regions, through complex interactions involving seasonal precipitation, scale mismatch, and vegetation density [50]. Its potentially greater influence towards the eastern Mediterranean [51] suggests that precipitation recycling may also be relevant to the study area and warrants further investigation.

Relative humidity showed negative relationships with both isotopes at all three stations, with the strongest relationships observed in Tetovo (R^2 = 0.7142 for $\delta^{18}O$ and 0.6793 for δ^2H), followed by Skopje (0.6814 and 0.6316) and Gevgelija (0.4832 and 0.3875) (Table 3). Pearson correlation analysis (Table 4) confirmed statistically significant negative correlations between relative humidity and $\delta^{18}O$ in Tetovo (r = −0.845, $p < 0.001$), Skopje (r = −0.825, $p < 0.001$), and Gevgelija (r = −0.695, p = 0.018). Similar significant negative correlations were observed for δ^2H, with r = −0.824 ($p < 0.001$), −0.795 (p = 0.001), and −0.623 (p = 0.041), respectively. These relationships suggest that humidity conditions influence precipitation isotopic composition through atmospheric moisture conditions, evaporation and condensation processes. Similar negative relationships have been reported in the Western Loess Plateau of China (slope −0.21‰ per RH percentage point) [52] and at most stations in the Tianshan Mountains of Central Asia [53], potentially reflecting sub-cloud evaporation and associated kinetic fractionation. In contrast, d-excess showed positive relationships with relative humidity at all three stations, with regression slopes ranging from 0.2556 (Tetovo) to 0.3337 (Gevgelija). The strongest relationship occurred in Tetovo (R^2 = 0.4783), followed by Skopje (0.4194) and Gevgelija (0.3140), indicating greater variability at the latter despite its steeper slope. Pearson correlation coefficients (Table 4) indicated positive correlations between relative humidity and d-excess in Tetovo (r = 0.692, p = 0.009), Skopje (r = 0.648, p = 0.017), and Gevgelija (r = 0.560, p = 0.073). These correlations were statistically significant in Tetovo and Skopje ($p < 0.05$), but not in Gevgelija. Similar positive associations have been reported along European coastal-to-inland transects and linked to regional rainout, continental effects and moisture trajectories [54]. Overall, these relationships indicate that relative humidity contributes to d-excess variability, reflecting differences in moisture uptake and transport, as well as seasonal atmospheric circulation and moisture sources [18,19].

Compared with temperature, precipitation amount and relative humidity, wind speed showed weaker and less consistent relationships with stable isotopes. The relationships were negligible in Tetovo (R^2 = 0.0047 for $\delta^{18}O$ and 0.0231 for δ^2H), moderate in Skopje (0.2319 and 0.1502, respectively), and comparable in Gevgelija (0.1529 and 0.1686), where both isotopes showed negative slopes (Table 3). Pearson correlation analysis (Table 4) showed weak and statistically non-significant correlations between wind speed and $\delta^{18}O$ in Tetovo (r = −0.069, p = 0.824), Skopje (r = 0.482, p = 0.096), and Gevgelija (r = −0.391,

p = 0.234). Similarly, the correlations with δ^2H were not statistically significant at any station, with r = −0.152 (p = 0.620), 0.388 (p = 0.191), and −0.411 (p = 0.210), respectively. The contrasting slope directions among stations suggest that wind influence depends on local meteorological conditions, air-mass origin and atmospheric circulation. Similarly, Kaseke et al. [55] reported a weak relationship between wind speed and $\delta^{18}O$ (R^2 = 0.06). The relationship between wind speed and d-excess was negative in Tetovo and Skopje (slopes −2.9608 and −3.2219, respectively), with a stronger relationship in Skopje (R^2 = 0.4975) than in Tetovo (0.1194). In contrast, Gevgelija showed a slight positive relationship (slope = 0.4251; R^2 = 0.0134). Pearson correlation coefficients (Table 4) indicated negative correlations between wind speed and d-excess in Tetovo (r = −0.346, p = 0.248) and Skopje (r = −0.705, p = 0.007), with only the latter being statistically significant. In Gevgelija, the correlation was negligible and statistically non-significant (r = 0.116, p = 0.735). Although d-excess is generally expected to increase with wind speed, seasonal conditions may produce negative relationships, as reported in Mediterranean coastal networks, including Egypt [56]. These contrasting results indicate that wind speed is not a consistent predictor of isotopic variability and that its influence should be interpreted in relation to local atmospheric conditions and moisture transport pathways.

Table 4. Pearson correlation coefficients (r) between precipitation isotopes, d-excess, and meteorological parameters, with two-tailed p-values in parentheses.

	$\delta^{18}O$ r (p)	**δ^2H r (p)**	**d-excess r (p)**
		Tetovo	
P	−0.744 (0.004)	−0.757 (0.003)	+0.462 (0.112)
T	+0.850 (<0.001)	+0.830 (<0.001)	−0.692 (0.009)
W	−0.069 (0.824)	−0.152 (0.620)	−0.346 (0.248)
Ap	+0.135 (0.660)	+0.217 (0.477)	+0.291 (0.334)
RH	−0.845 (<0.001)	−0.824 (<0.001)	+0.692 (0.009)
		Skopje	
P	−0.661 (0.014)	−0.668 (0.013)	+0.386 (0.193)
T	+0.875 (<0.001)	+0.842 (<0.001)	−0.687 (0.010)
W	+0.482 (0.096)	+0.388 (0.191)	−0.705 (0.007)
Ap	−0.188 (0.539)	−0.072 (0.816)	+0.616 (0.025)
RH	−0.825 (<0.001)	−0.795 (0.001)	+0.648 (0.017)
		Gevgelija	
P	−0.658 (0.028)	−0.607 (0.048)	+0.470 (0.144)
T	+0.788 (0.004)	+0.710 (0.014)	−0.622 (0.041)
W	−0.391 (0.234)	−0.411 (0.210)	+0.116 (0.735)
Ap	−0.047 (0.891)	+0.107 (0.753)	+0.531 (0.093)
RH	−0.695 (0.018)	−0.623 (0.041)	+0.560 (0.073)

Although stable isotopes may show positive relationships with atmospheric pressure [57], reflecting its influence on atmospheric circulation and moisture transport, pressure exhibited generally weak relationships with $\delta^{18}O$ and δ^2H at all three stations. The R^2 values ranged from 0.0022 to 0.0352 for $\delta^{18}O$ and from 0.0051 to 0.0470 for δ^2H, indicating negligible explanatory power, as shown in Table 3. Pearson correlation analysis (Table 4) confirmed weak and statistically non-significant correlations between atmospheric pressure and $\delta^{18}O$ in Tetovo (r = 0.135, p = 0.660), Skopje (r = −0.188, p = 0.539), and Gevgelija (r = −0.047, p = 0.891). Similarly, the correlations with δ^2H were not statistically significant, with r = 0.217 (p = 0.477), −0.072 (p = 0.816), and 0.107 (p = 0.753), respectively. Previous studies have also reported weak or absent relationships between precipitation isotopes and local atmospheric pressure, emphasizing the greater influence of moisture sources

and atmospheric circulation [58,59]. In contrast, d-excess showed positive relationships with atmospheric pressure at all stations, with the strongest relationships in Skopje (R^2 = 0.3798) and Gevgelija (0.2818), and a weaker one in Tetovo (0.0849). The regression slopes were 0.5408, 1.1559 and 1.1254, respectively. Pearson correlation coefficients (Table 4) indicated positive correlations between atmospheric pressure and d-excess in Tetovo (r = 0.291, p = 0.334), Skopje (r = 0.616, p = 0.025), and Gevgelija (r = 0.531, p = 0.093). However, only the correlation in Skopje was statistically significant ($p < 0.05$). These results suggest that pressure may indirectly reflect changes in atmospheric circulation and moisture transport rather than directly control isotopic fractionation. The importance of moisture origin for precipitation d-excess has also been highlighted by Türk et al. [27].

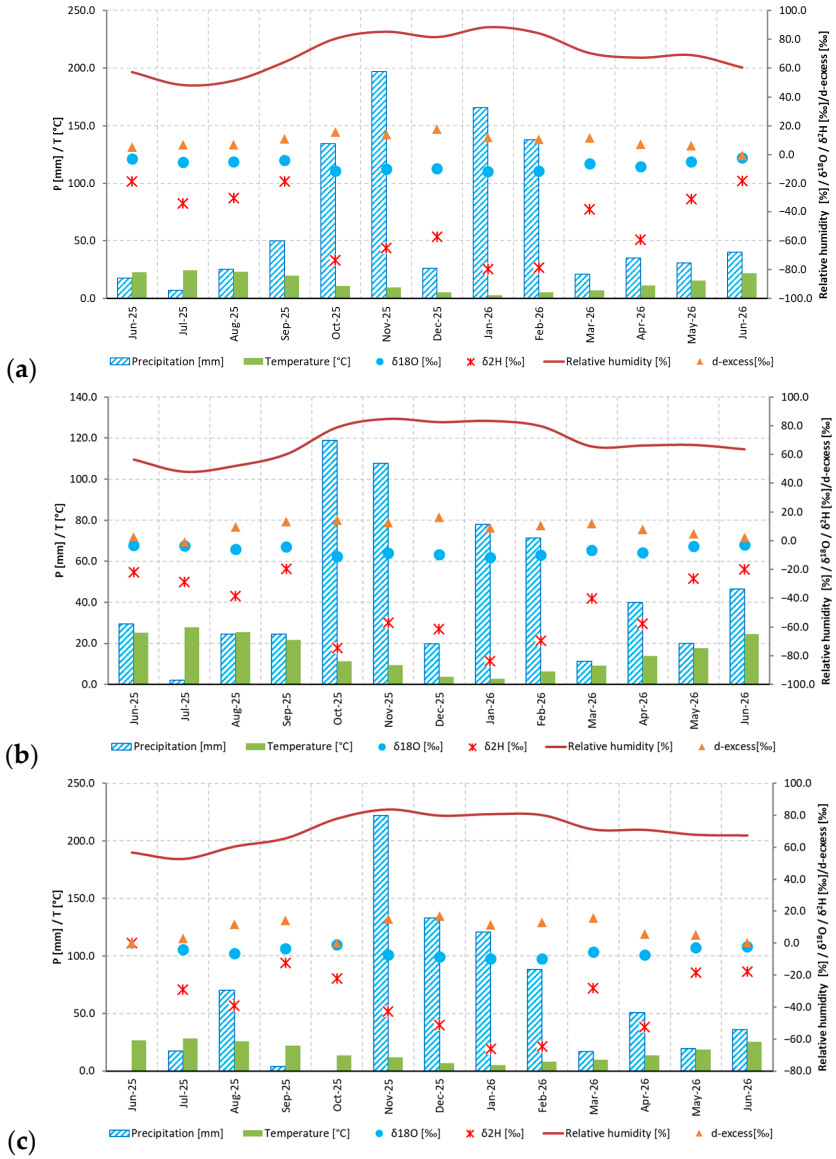

Figure 3. Temporal variations/comparison between: precipitation amount P [mm], air temperature T [°C], relative humidity RH [%], isotopic composition of precipitation $\delta^{18}O$ and $\delta^{2}H$ [‰] and d-excess [‰] for 3 sampling sites: (**a**) Tetovo, (**b**) Skopje, (**c**) Gevgelija.

Overall, regression and Pearson correlation analyses identified air temperature as the meteorological parameter most consistently associated with precipitation isotopic composition, followed by relative humidity and precipitation amount. Positive relationships with temperature indicate isotopic enrichment during warmer periods, while negative re-

lationships with precipitation amount and relative humidity reflect the influence of precipitation and atmospheric moisture conditions. Wind speed and atmospheric pressure showed weaker and less consistent associations with $\delta^{18}O$ and $\delta^{2}H$, although statistically significant relationships with d-excess were identified in Skopje. In contrast, d-excess generally exhibited negative relationships with temperature and positive relationships with relative humidity and precipitation amount, providing complementary information on moisture conditions, evaporation and potential changes in moisture sources. Differences among the three stations highlight the combined influence of regional climate and local environmental conditions on precipitation isotope variability. From an environmental perspective, these findings demonstrate the value of stable isotopes as indicators of seasonal atmospheric and hydrometeorological variability, supporting further investigations of water sources and hydrological processes in the Vardar River basin.

4.4. LMWL

The relationship between $\delta^{18}O$ and $\delta^{2}H$ in precipitation is represented by the Global Meteoric Water Line (GMWL), defined by Craig as $\delta^{2}H = 8 \times \delta^{18}O + 10$ [1]. This equation was updated by Rozanski et al. [4] and subsequently by Araguás-Araguás et al. [37], resulting in the form $\delta^{2}H = 7.96 \times \delta^{18}O + 8.86$. The slope of the line reflects the degree of O and H fractionation and is highly sensitive to evaporation from moisture sources [60], the evaporation of raindrops below the clouds as they fall through layers of unsaturated air [61,62], as well as the mixing of multiple moisture sources [63]. To characterize precipitation isotope relationships under the local environmental conditions of the measuring stations, Local Meteoric Water Lines (LMWLs) were established for Tetovo, Skopje, and Gevgelija, as shown in Figure 4.

The Local Meteoric Water Lines (LMWLs) exhibited strong linear relationships between $\delta^{18}O$ and $\delta^{2}H$, with coefficients of determination (R^2) ranging from 0.9375 to 0.9803.

$$\text{Tetovo: } \delta^{2}H = 6.8639 \times \delta^{18}O + 1.9445 \ (R^2 = 0.9803) \quad (1)$$

$$\text{Skopje: } \delta^{2}H = 6.8525 \times \delta^{18}O + 1.1671 \ (R^2 = 0.9714) \quad (2)$$

$$\text{Gevgelija: } \delta^{2}H = 6.7609 \times \delta^{18}O + 2.885 \ (R^2 = 0.9375) \quad (3)$$

In addition to the individual LMWLs, a Regional Meteoric Water Line (RMWL) was established using the combined precipitation isotope data from Tetovo, Skopje, and Gevgelija to characterize the overall $\delta^{18}O$–$\delta^{2}H$ relationship across the Vardar River basin (Figure 5). The resulting regression equation was:

$$\text{RMWL: } \delta^{2}H = 6.8734 \times \delta^{18}O + 2.2294 \ (R^2 = 0.9666) \quad (4)$$

The strongest LMWL relationship was observed in Tetovo ($R^2 = 0.9803$), followed by Skopje (0.9714) and Gevgelija (0.9375). The calculated slopes ranged from 6.7609 to 6.8639, considerably below the GMWL slope of 7.96, suggesting kinetic isotopic fractionation, potentially associated with sub-cloud evaporation under unsaturated atmospheric conditions [19]. Despite minor spatial differences, the relatively narrow slope range indicates similar isotopic relationships across the three stations, potentially influenced by atmospheric humidity, moisture sources and seasonal climatic variability. The LMWL intercepts also varied spatially, ranging from 1.1671‰ in Skopje to 2.885‰ in Gevgelija, all substantially below the GMWL intercept of 8.86‰. The different slope and intercept patterns suggest that LMWL characteristics are influenced not only by evaporation but also by atmospheric circulation, moisture sources and regional environmental conditions. Overall, the lower slopes and intercepts compared with the GMWL highlight the influence of regional atmospheric processes on precipitation isotope composition. Similar deviations of local

meteoric water lines from the GMWL have been reported in previous studies conducted in Mediterranean and adjacent regions [64,65]. These findings are consistent with the relatively low LMWL slopes and intercepts observed in Tetovo, Skopje, and Gevgelija, suggesting that regional atmospheric conditions and nonequilibrium isotopic fractionation processes may influence precipitation isotope composition across the study area. The seasonal distribution of precipitation isotopes at Tetovo, Skopje, and Gevgelija exhibits distinct variations in relation to the Global Meteoric Water Line (GMWL) and the corresponding Local Meteoric Water Lines (LMWLs), as illustrated in Figure 4. At all three stations, summer precipitation is generally isotopically enriched and plots below both reference lines, whereas winter precipitation is more depleted, reflecting the seasonal influence of climatic and atmospheric conditions on precipitation isotope signatures. Similar seasonal patterns were reported by Natali et al. [66] in Tuscany, Italy, where variations in precipitation isotope composition were associated with changes in local meteorological conditions and atmospheric moisture transport throughout the year.

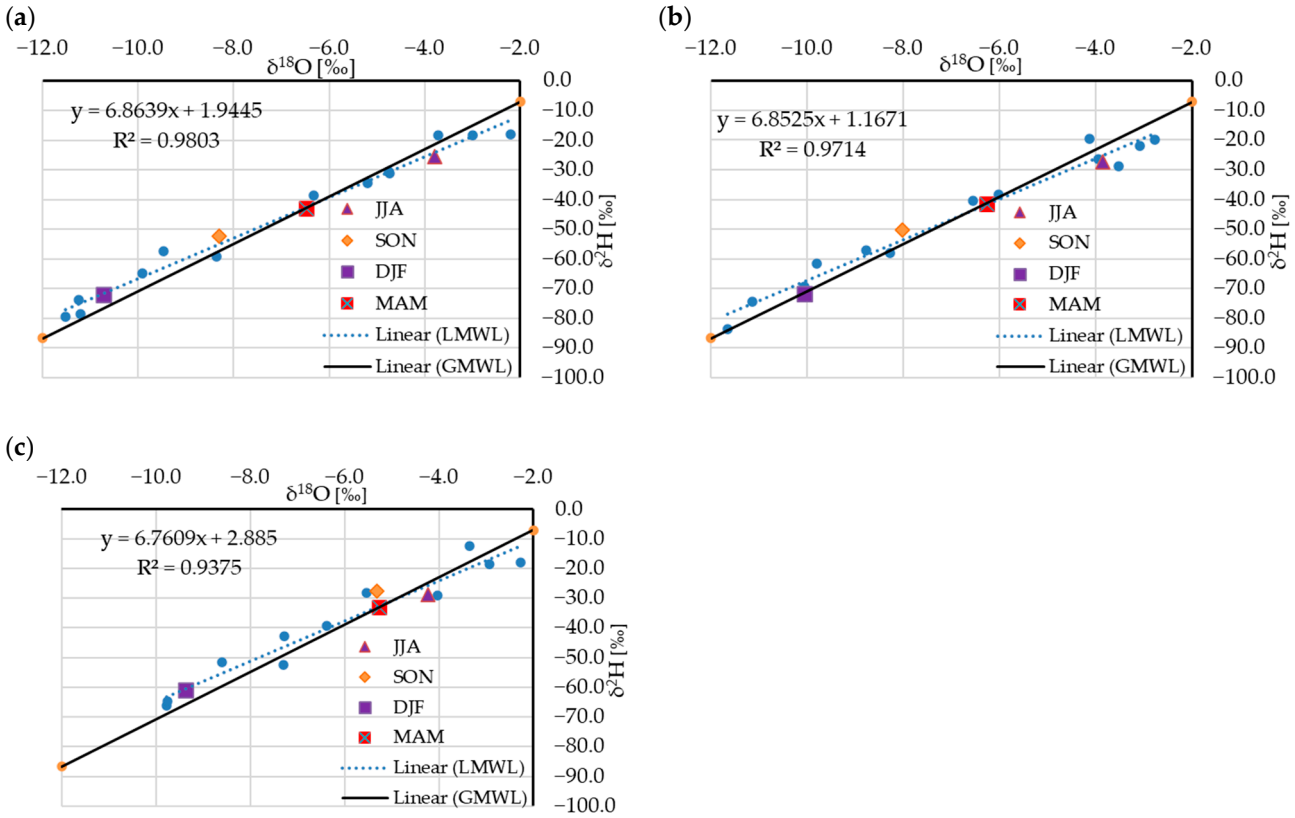

Figure 4. The Local Meteoric Water Lines (LMWLs) derived from precipitation data (represented by blue dots), together with seasonal precipitation data, compared to the Global Meteoric Water Line (GMWL): (**a**) Tetovo, (**b**) Skopje, (**c**) Gevgelija.

At Tetovo, winter and autumn (SON) samples plot above both the GMWL and LMWL, while spring (MAM) samples occur near their intersection. At Skopje, winter precipitation is positioned close to the GMWL and slightly below the LMWL, whereas autumn samples plot above both lines and spring samples plot near their intersection. At Gevgelija, winter and autumn samples plot above both reference lines, while spring samples occur below the GMWL and close to the LMWL. These differences indicate that, despite broadly similar seasonal patterns, the positions of precipitation isotope values relative to the meteoric water lines vary among stations. The relatively enriched summer val-

ues and their positions below the GMWL may reflect evaporation-related isotopic fractionation, whereas the generally higher positions of autumn and winter values suggest seasonal changes in d-excess, atmospheric moisture conditions, and moisture-source characteristics. Comparable seasonal variations have been reported in Croatia and Italy [67–69], where lower summer d-excess and higher autumn–winter values were associated with evaporation-related processes and changes in atmospheric moisture transport. Overall, these findings highlight the influence of seasonal climatic variability and regional environmental conditions on precipitation isotope composition across the Vardar River basin. Overall, the three monitoring stations exhibit comparable seasonal isotopic distributions, characterized by relatively enriched summer precipitation and depleted winter precipitation.

The seasonal positions relative to the GMWL and LMWLs indicate differences in isotopic characteristics throughout the year, with summer precipitation generally plotting below the GMWL and autumn precipitation above it. These patterns, together with the consistently reduced LMWL slopes, suggest the influence of seasonal atmospheric and environmental conditions, potentially including secondary evaporation, variations in humidity, and changes in moisture sources and transport pathways. The observed seasonal patterns are consistent with previous investigations in Mediterranean and southeastern European regions [65–69], which emphasize the combined influence of local meteorological conditions, atmospheric moisture transport, and isotopic fractionation processes on seasonal precipitation isotope variability.

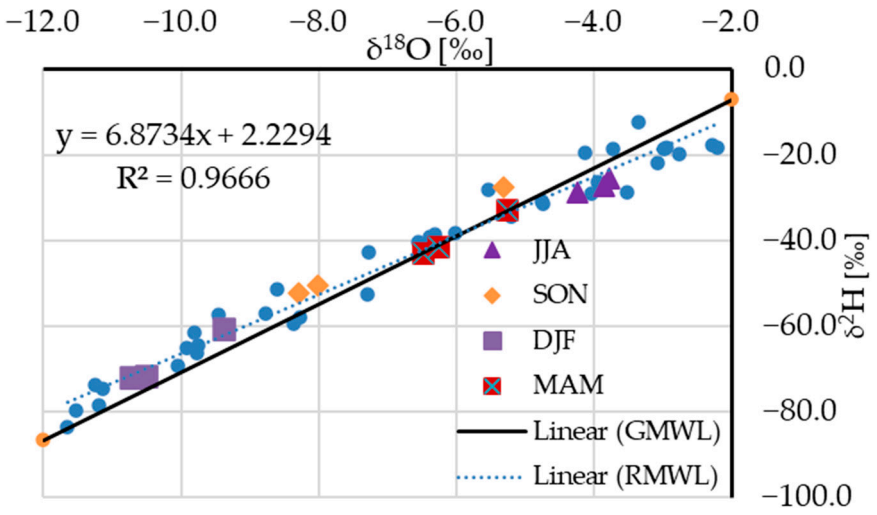

Figure 5. The Regional Meteoric Water Line (RMWL) derived from combined precipitation data from the three monitoring stations (represented by blue dots), together with seasonal precipitation data, compared to the Global Meteoric Water Line (GMWL).

The Regional Meteoric Water Line (RMWL), established using the combined precipitation isotope data from the three monitoring stations, exhibited a strong linear relationship ($\delta^2H = 6.8734 \times \delta^{18}O + 2.2294$; $R^2 = 0.9666$). Its slope was comparable to those of the LMWLs established for Tetovo (6.8639), Skopje (6.8525), and Gevgelija (6.7609), indicating broadly similar $\delta^{18}O$–δ^2H relationships across the Vardar River basin. The RMWL slope was slightly lower than that of Tetovo but higher than those of Skopje and Gevgelija, while its intercept fell within the range of the individual LMWL intercepts (1.1671–2.8850‰). All four meteoric water lines exhibited slopes and intercepts below those of the GMWL, suggesting a consistent regional influence of atmospheric moisture conditions and potentially evaporation-related isotopic fractionation processes. The relatively small differences

between the RMWL and LMWLs indicate limited spatial variability in the overall precipitation isotope relationships among the three stations.

5. Conclusions

This study investigated the seasonal and spatial variability of stable oxygen ($\delta^{18}O$) and hydrogen ($\delta^{2}H$) isotopes in precipitation across the Vardar River basin, North Macedonia, based on observations from Tetovo, Skopje, and Gevgelija between June 2025 and June 2026. The results provide insights into the influence of seasonal climate, meteorological conditions, and elevation on precipitation isotope composition.

A consistent seasonal pattern was observed at all three monitoring stations, with isotopic enrichment during summer and depletion during winter. Mean $\delta^{18}O$ values were −7.05‰, −6.90‰, and −6.11‰, while $\delta^{2}H$ values were −46.4‰, −46.1‰, and −38.4‰ in Tetovo, Skopje, and Gevgelija, respectively. Gevgelija showed the most enriched composition and lowest temporal variability, highlighting spatial differences in precipitation isotope characteristics. Spatial interpolation and elevation-based regression indicated more depleted isotopic values in mountainous areas and enrichment at lower elevations, particularly along the Vardar River valley. Although elevation appears to influence regional isotope distribution, further validation using additional monitoring stations, especially at higher elevations, is needed. Among the meteorological parameters, air temperature showed the strongest and most consistent positive relationships with $\delta^{18}O$ and $\delta^{2}H$, while relative humidity and precipitation amount exhibited negative associations. Wind speed showed weaker and variable relationships, whereas atmospheric pressure had minimal explanatory power. These findings highlight the combined influence of seasonal climatic and atmospheric conditions on precipitation isotope variability. The established Local Meteoric Water Lines showed strong relationships between $\delta^{18}O$ and $\delta^{2}H$, with slopes of 6.86, 6.85, and 6.76 for Tetovo, Skopje, and Gevgelija, respectively (R^2 = 0.94–0.98). Their lower slopes compared with the Global Meteoric Water Line suggest the influence of nonequilibrium fractionation processes. Seasonal d-excess variability, with higher values during autumn and winter and lower values during summer, further indicates the influence of changing atmospheric moisture conditions and potential secondary evaporation. Its relatively weak relationship with elevation (annual R^2 = 0.2515) confirms that altitude alone cannot explain its spatial variability.

Overall, this study provides an important contribution to understanding precipitation isotope variability and its environmental controls in the Vardar River basin. Despite the relatively short monitoring period and limited spatial coverage, the results establish a basis for further multi-year isotope monitoring, investigation of atmospheric moisture transport, and improved regional isotope characterization. Expanding the monitoring network across different elevations will support future groundwater recharge assessments and sustainable water resource management.

Author Contributions: Conceptualization, V.G. and B.I.; methodology, V.G.; validation, V.G., B.I. and Z.K.; sample collection, V.G. and B.I.; sample preparation and interpretation, Z.K.; stable isotope measurement, Z.K.; data curation, V.G., B.I. and Z.K.; writing—original draft preparation, V.G. and B.I.; visualization, V.G. and B.I.; supervision, Z.K.; communicating with the journal, V.G.; funding acquisition, V.G. All the co-authors participated in discussions and reviewed the manuscript. All authors have read and agreed to the published version of the manuscript.

Funding: This paper is the result of research conducted within the framework of a scientific research project: "Analysis of natural isotopes in precipitation, surface and groundwater", which is funded by the Ministry of Education and Science of the Republic of Macedonia.

Data Availability Statement: The original contributions presented in this study are included in the article. Further inquiries can be directed to the corresponding author.

Acknowledgments: We are thankful to Elena Paneva Gjorgievski and the staff at the Hydrometeorological Service of Macedonia for providing access to the HSM premises to install rain collectors for precipitation sampling. We are thankful to the staff at the Faculty of Civil Engineering Skopje for all the support in the ongoing project. We are grateful to the IAEA, which, within the framework of the RER7017: Ensuring Water Availability in a Changing Climate project, donated materials and equipment used for sampling and sample storage.

Conflicts of Interest: The authors declare no conflicts of interest. The funders had no role in the design of the study; in the collection, analyses, or interpretation of data; in the writing of the manuscript; or in the decision to publish the results.

Abbreviations

The following abbreviations are used in this manuscript:

GMWL	Global Meteoric Water Line
δ^2H	stable isotope of hydrogen (deuterium)
$\delta^{18}O$	stable isotope of oxygen
P	Precipitation
IAEA	International Atomic Energy Agency
HSM	Hydrometeorological Service of Macedonia
VSMOW	Vienna Standard Mean Ocean Water
LIMS	Laboratory Information Management System
SMOW	Standard Mean Ocean Water
LMWL	Local Meteoric Water Line
RMWL	Regional Meteoric Water Line
LWIA	Liquid Water Isotope Analyzer
LGR	Los Gatos Research

Appendix A. Data of Stable Isotopes

Table A1. The isotope composition (δ^2H and $\delta^{18}O$ values) of precipitation and d-excess in Tetovo.

ID	Month	Collection Date	δ^2H, in ‰	$\delta^{18}O$, in ‰	d-excess
1	Jun 2025	4 July 2025	−18.5	−2.99	5.3
2	Jul 2025	1 August 2025	−34.4	−5.20	7.0
3	Aug 2025	29 August 2025	−30.7	−4.75	7.1
4	Sep 2025	29 September 2025	−18.5	−3.72	11.1
5	Oct 2025	29 October 2025	−73.7	−11.25	15.9
6	Nov 2025	3 December 2025	−65.0	−9.92	14.0
7	Dec 2025	26 December 2025	−57.4	−9.46	17.9
8	Jan 2026	3 February 2026	−79.6	−11.53	12.2
9	Feb 2026	27 February 2026	−78.6	−11.20	10.6
10	Mar 2026	30 Mart 2026	−38.6	−6.32	11.7
11	Apr 2026	29 April 2026	−59.3	−8.36	7.3
12	May 2026	28 May 2026	−31.3	−4.74	6.4
13	Jun 2026	6 June 2026	−18.2	−2.21	−0.6

Table A2. The isotope composition (δ^2H and $\delta^{18}O$ values) of precipitation and d-excess in Skopje.

ID	Month	Collection Date	δ^2H, in ‰	$\delta^{18}O$, in ‰	d-excess
1	Jun 2025	4 July 2025	−21.9	−3.08	2.6

2	Jul 2025	1 August 2025	−28.8	−3.52	−0.8
3	Aug 2025	1 September 2025	−38.4	−6.02	9.5
4	Sep 2025	1 October 2025	−19.5	−4.13	13.4
5	Oct 2025	31 October 2025	−74.5	−11.14	14.2
6	Nov 2025	3 December 2025	−57.2	−8.78	12.7
7	Dec 2025	26 December 2025	−61.6	−9.80	16.4
8	Jan 2026	3 February 2026	−83.7	−11.65	9.0
9	Feb 2026	27 February 2026	−69.4	−10.05	10.6
10	Mar 2026	30 Mart 2026	−40.3	−6.55	11.8
11	Apr 2026	6 May 2026	−57.9	−8.27	7.9
12	May 2026	28 May 2026	−26.5	−3.94	4.9
13	Jun 2026	6 July 2026	−19.8	−2.77	2.3

Table A3. The isotope composition (δ^2H and $\delta^{18}O$ values) of precipitation and d-excess in Gevgelija.

ID	Month	Collection Date	δ^2H, in ‰	$\delta^{18}O$, in ‰	d-excess
1	Jun 2025				
2	Jul 2025	1 August 2025	−29.0	−4.03	3.1
3	Aug 2025	1 September 2025	−39.2	−6.39	11.7
4	Sep 2025	30 September 2025	−12.4	−3.35	14.3
5 *	Oct 2025	31 October 2025	−22.0	−0.92	−14.7
6	Nov 2025	1 December 2025	−42.9	−7.28	15.1
7	Dec 2025	29 December 2025	−51.4	−8.60	17.1
8	Jan 2026	2 February 2026	−66.3	−9.77	11.5
9	Feb 2026	2 Mart 2026	−64.6	−9.75	13.0
10	Mar 2026	31 Mart 2026	−28.3	−5.54	15.8
11	Apr 2026	4 May 2026	−52.5	−7.30	5.6
12	May 2026	27 May 2026	−18.4	−2.94	5.0
13	Jun 2026	6 July 2026	−17.8	−2.28	0.4

* The sample analysis was not used in the analysis.

Table A4. Relationship between stable isotope content and d-excess in precipitation and elevation and estimated vertical gradient.

	$\delta^{18}O$-Elevation	Vertical Gradient [‰/100 m]	δ^2H-Elevation	Vertical Gradient [‰/100 m]	d-excess-Elevation	Vertical Gradient [‰/100 m]
JJA	$\delta^{18}O = 0.0012 \times H - 4.2698$ ($R^2 = 0.9331$)	0.12	$\delta^2H = 0.008 \times H - 29.265$ ($R^2 = 0.9617$)	0.8	d-excess $= -0.0014 \times H + 4.7545$ ($R^2 = 0.1042$)	−0.1
SON	$\delta^{18}O = -0.0079 \times H - 5.0794$ ($R^2 = 0.9113$)	−0.79	$\delta^2H = -0.0658 \times H - 25.726$ ($R^2 = 0.9041$)	−6.6	d-excess $= -0.0028 \times H + 14.666$ ($R^2 = 0.7107$)	−0.3
DJF	$\delta^{18}O = -0.0036 \times H - 9.237$ ($R^2 = 0.9485$)	−0.36	$\delta^2H = -0.0297 \times H - 60.042$ ($R^2 = 0.8733$)	−3.0	d-excess $= -0.0014 \times H + 13.521$ ($R^2 = 0.084$)	−0.1
MAM	$\delta^{18}O = -0.0032 \times H - 5.1382$ ($R^2 = 0.954$)	−0.32	$\delta^2H = -0.0263 \times H - 32.135$ ($R^2 = 0.9397$)	−2.6	d-excess $= -0.001 \times H + 8.7634$ ($R^2 = 0.0.4621$)	−0.1
Winter	$\delta^{18}O = -0.0044 \times H - 7.8812$ ($R^2 = 0.9419$)	−0.44	$\delta^2H = -0.0362 \times H - 49.942$ ($R^2 = 0.9042$)	−3.6	d-excess $= -0.001 \times H + 12.793$ ($R^2 = 0.0975$)	−0.1
summer	$\delta^{18}O = -0.0004 \times H - 3.7842$ ($R^2 = 0.9543$)	−0.04	$\delta^2H = -0.0054 \times H - 23.371$ ($R^2 = 0.6791$)	−0.5	d-excess $= -0.0025 \times H + 6.7479$ ($R^2 = 0.3971$)	−0.3
Annual	$\delta^{18}O = -0.0025 \times H - 6.0201$ ($R^2 = 0.9442$)	−0.25	$\delta^2H = -0.0214 \times H - 37.885$ ($R^2 = 0.8831$)	−2.1	d-excess $= -0.0018 \times H + 10.045$ ($R^2 = 0.2515$)	−0.2

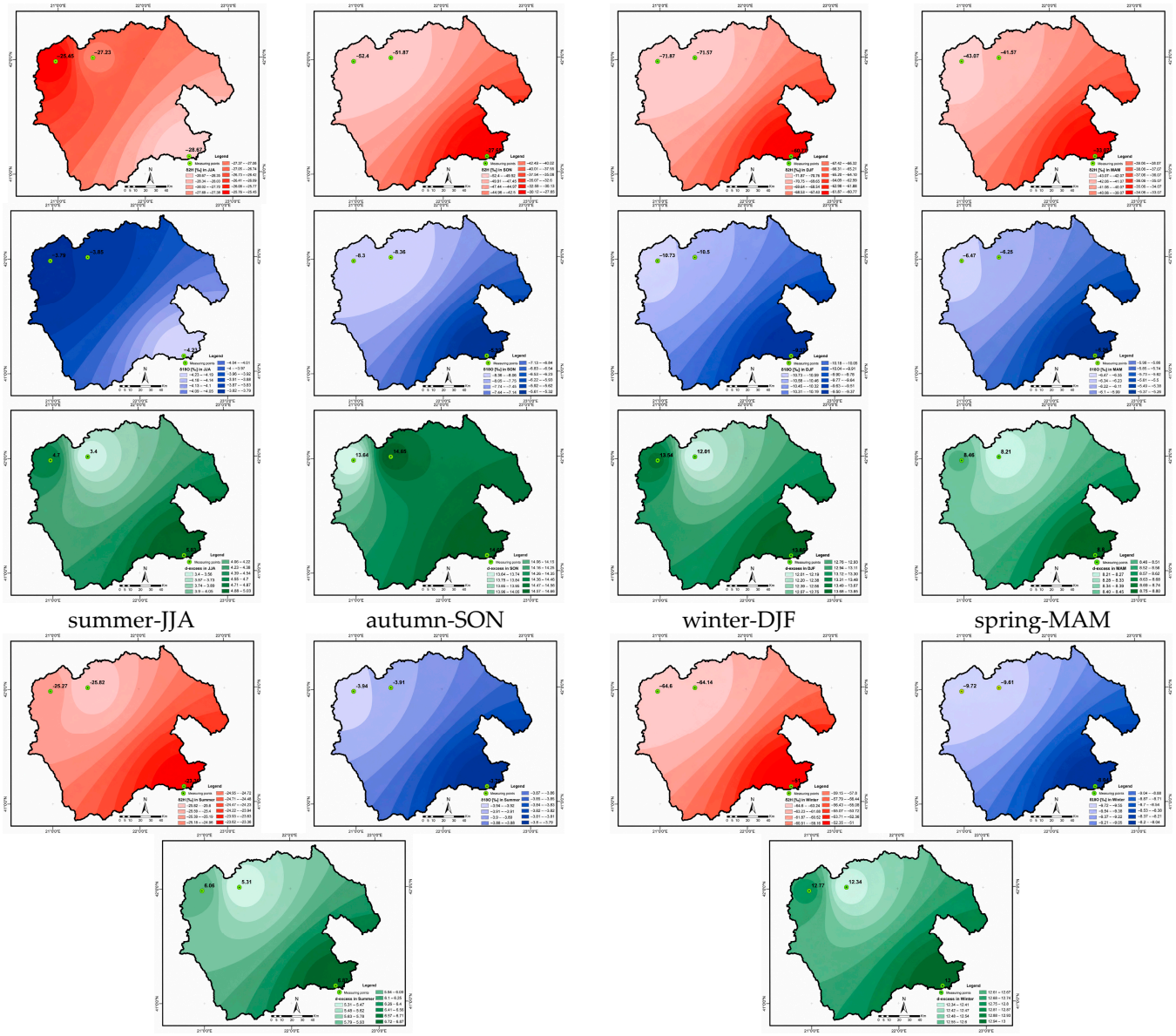

Figure A1. Spatial variability of isotopes in precipitation by season-IDW method (the distribution of oxygen is shown in blue, the distribution of hydrogen in red, and the distribution of d-excess in green).

https://doi.org/10.3390/environments13120659

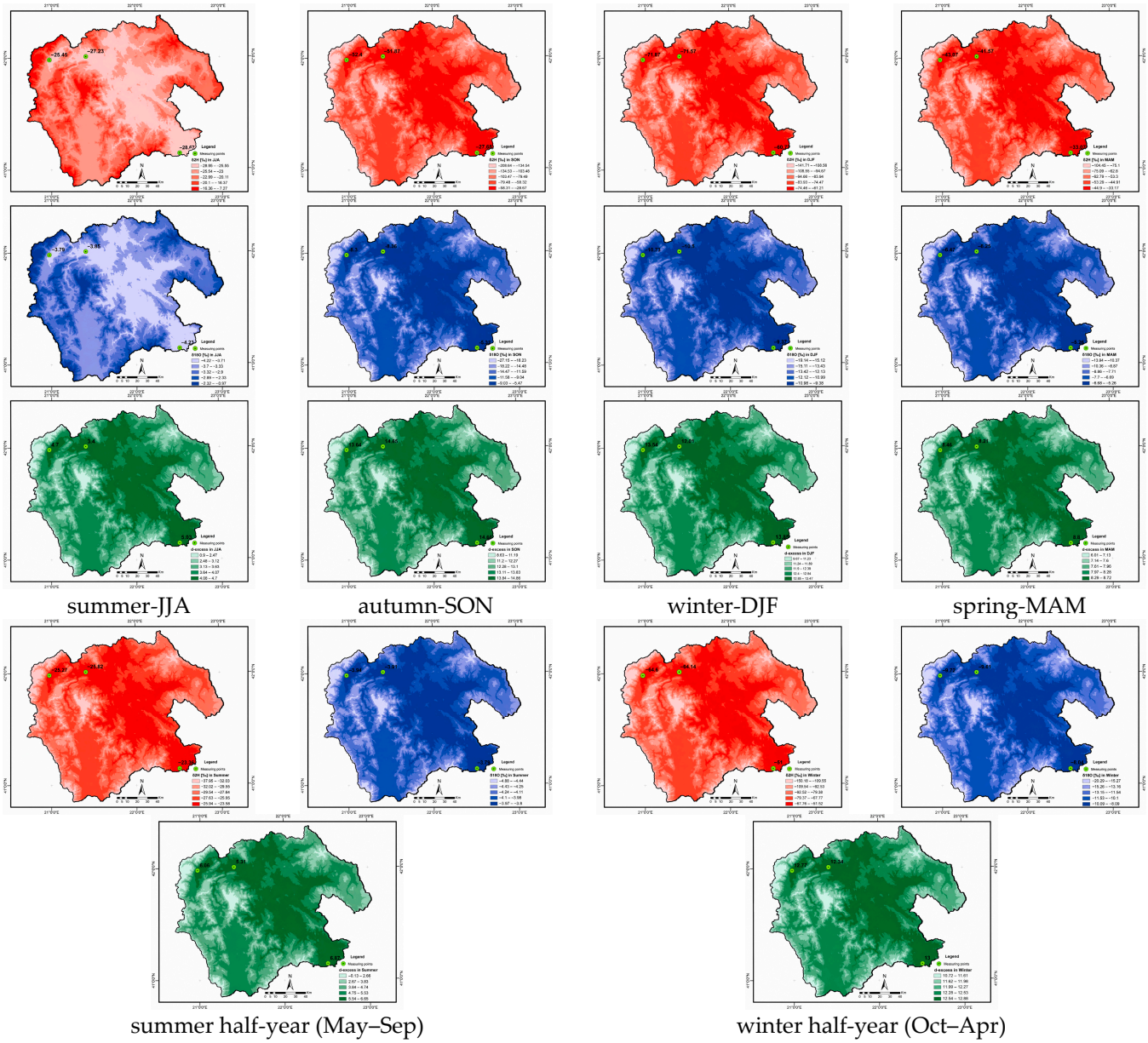

Figure A2. Spatial variability of isotopes in precipitation by season—Elevation-based regression model (the distribution of oxygen is shown in blue, the distribution of hydrogen in red, and the distribution of d-excess in green).

Appendix B. Meteorological and Isotopic Relationships



Figure A3. Relationship between stable isotope content and d-excess in precipitation and climatic parameters in Tetovo: (**a**) relationship between $\delta^{18}O$ and precipitation amount/temperature/wind speed/atmospheric pressure/relative humidity, (**b**) relationship between $\delta^{2}H$ and precipitation amount/temperature/wind speed/atmospheric pressure/relative humidity, (**c**) relationship between d-excess and precipitation amount/temperature/wind speed/atmospheric pressure/relative humidity.

https://doi.org/10.3390/environments13120659

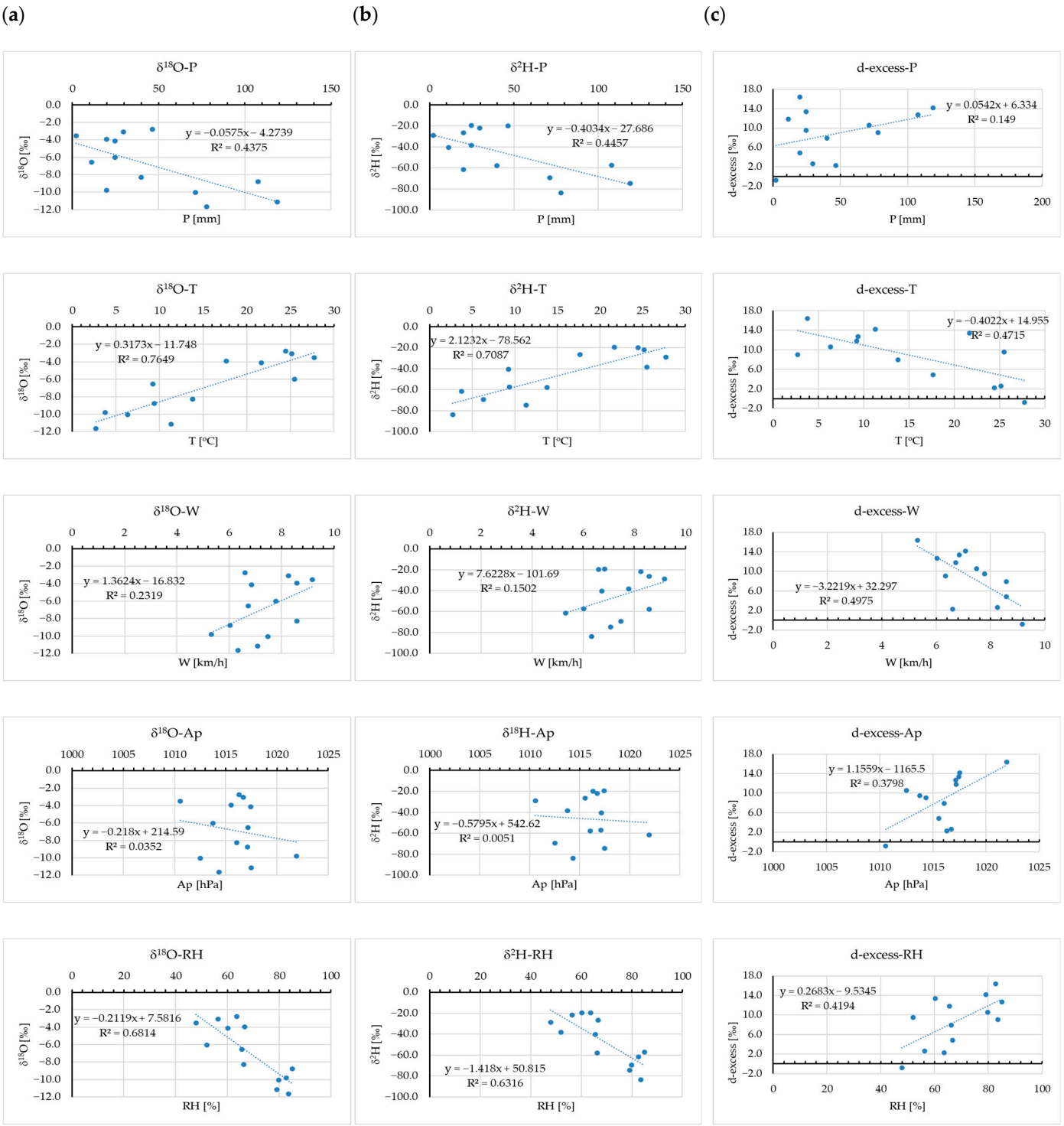

Figure A4. Relationship between stable isotope content and d-excess in precipitation and climatic parameters in Skopje: (**a**) relationship between $\delta^{18}O$ and precipitation amount/temperature/wind speed/atmospheric pressure/relative humidity, (**b**) relationship between $\delta^{2}H$ and precipitation amount/temperature/wind speed/atmospheric pressure/relative humidity, (**c**) relationship between d-excess and precipitation amount/temperature/wind speed/atmospheric pressure/relative humidity.

https://doi.org/10.3390/environments13120659

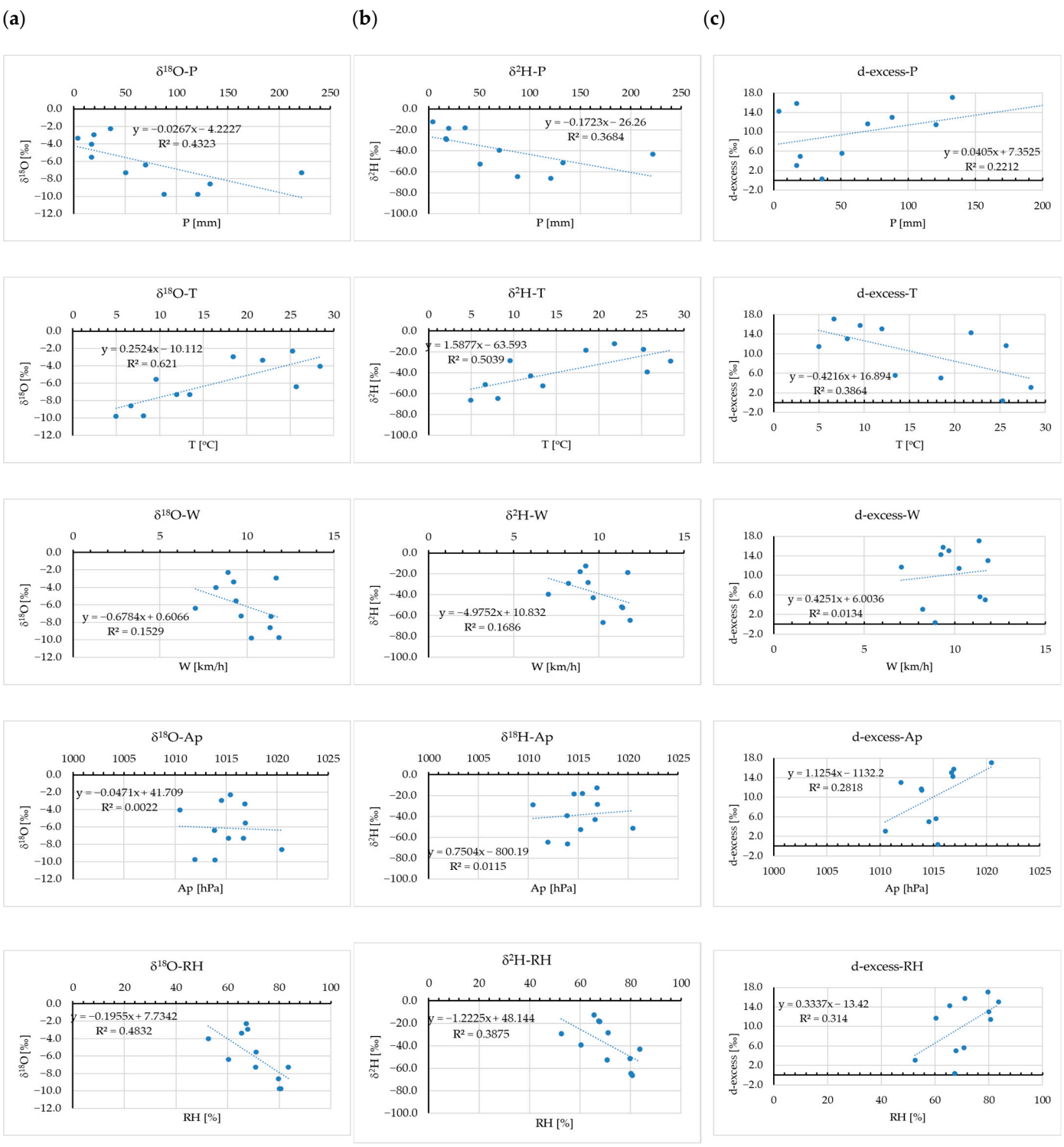

Figure A5. Relationship between stable isotope content and d-excess in precipitation and climatic parameters in Gevgelija: (**a**) relationship between $\delta^{18}O$ and precipitation amount/temperature/wind speed/atmospheric pressure/relative humidity, (**b**) relationship between $\delta^{2}H$ and precipitation amount/temperature/wind speed/atmospheric pressure/relative humidity, (**c**) relationship between d-excess and precipitation amount/temperature/wind speed/atmospheric pressure/relative humidity.

References

1. Craig, H. Isotopic Variations in Meteoric Waters. *Science* **1961**, *133*, 1702–1703. https://doi.org/10.1126/science.133.3465.1702.
2. Dansgaard, W. Stable Isotopes in Precipitation. *Tellus* **1964**, *16*, 436–468. https://doi.org/10.3402/tellusa.v16i4.8993.
3. Gat, J.R. Oxygen and Hydrogen Isotopes in the Hydrologic Cycle. *Annu. Rev. Earth Planet. Sci.* **1996**, *24*, 225–262. https://doi.org/10.1146/annurev.earth.24.1.225.
4. Rozanski, K.; Araguás-Araguás, L.; Gonfiantini, R. Isotopic Patterns in Modern Global Precipitation. In *Climate Change in Continental Isotopic Records*; American Geophysical Union: Washington, DC, USA, 1993; Volume 78, pp. 1–36. https://doi.org/10.1029/GM078p0001.
5. Jasechko, S. Global Isotope Hydrogeology—Review. *Rev. Geophys.* **2019**, *57*, 835–965. https://doi.org/10.1029/2018RG000627.
6. Clark, I.D.; Fritz, P. *Environmental Isotopes in Hydrogeology*; CRC Press/Lewis Publishers: Boca Raton, FL, USA, 1997.
7. Bowen, G.J.; Wilkinson, B. Spatial Distribution of $\delta^{18}O$ in Meteoric Precipitation. *Geology* **2002**, *30*, 315–318. https://doi.org/10.1130/0091-7613(2002)030<0315:SDOOIM>2.0.CO;2.
8. Aggarwal, P.K.; Alduchov, O.A.; Froehlich, K.O.; Araguás-Araguás, L.J.; Sturchio, N.C.; Kurita, N. Stable Isotopes in Global Precipitation: A Unified Interpretation Based on Atmospheric Moisture Residence Time. *Geophys. Res. Lett.* **2012**, *39*, L11705. https://doi.org/10.1029/2012GL051937.
9. Rozanski, K.; Sonntag, C.; Münnich, K.O. Factors Controlling Stable Isotope Composition of European Precipitation. *Tellus* **1982**, *34*, 142–150. https://doi.org/10.3402/tellusa.v34i2.10796.
10. Feng, X.; Faiia, A.M.; Posmentier, E.S. Seasonality of Isotopes in Precipitation: A Global Perspective. *J. Geophys. Res. Atmos.* **2009**, *114*, D08116. https://doi.org/10.1029/2008JD011279.
11. Lan, X.; Jia, W.; Zhu, G.; Zhang, Y.; Yu, Z.; Luo, H. Spatial and Temporal Variation Characteristics of Stable Isotopes in Precipitation and Their Relationships with Meteorological Factors in the Shiyang River Basin in China. *Water* **2023**, *15*, 3836. https://doi.org/10.3390/w15213836.
12. Zhu, H.; Zhu, L.; Luo, L.; Li, J. Seasonal Variations of Modern Precipitation Stable Isotopes over the North Tibetan Plateau and Their Influencing Factors. *Water* **2024**, *16*, 150. https://doi.org/10.3390/w16010150.
13. Zhang, J.; Yu, W.; Lewis, S.; Thompson, L.G.; Bowen, G.J.; Yoshimura, K.; Cauquoin, A.; Werner, M.; Chakraborty, S.; Jing, Z.; et al. Controls on Stable Water Isotopes in Monsoonal Precipitation Across the Bay of Bengal: Atmosphere and Surface Analysis. *Geophys. Res. Lett.* **2023**, *50*, e2022GL102229. https://doi.org/10.1029/2022GL102229.
14. Bekaert, D.V.; Longeau, A.; Risi, C.; Fénisse, G.; Prud'Homme, C.; Ram, R.; Zhang, J.; Genty, D.; Seltzer, A.M.; Aeschbach, W.; et al. Temperature-Sensitivity of Water Stable Isotopes in Global Precipitation: A Groundwater Noble Gas-Based, Paleoclimate Perspective. *Adv. Geochem. Cosmochem.* **2026**, *2*, 1097. https://doi.org/10.33063/agc.v2i2.1097.
15. Casado, M.; Bailey, A.; Leroy-Dos Santos, C.; Fourré, E.; Favier, V.; Agosta, C.; Dutrievoz, N.; Kittel, C.; Arnaud, L.; Prié, F.; et al. Water Isotope–Temperature Relationship Variability across Antarctica Set by Atmospheric Circulation. *Nat. Geosci.* **2026**, *19*, 581–588. https://doi.org/10.1038/s41561-026-01961-y.
16. Putman, A.L.; Fiorella, R.P.; Bowen, G.J.; Cai, Z. A Global Perspective on Local Meteoric Water Lines: Meta-Analytic Insight into Fundamental Controls and Practical Constraints. *Water Resour. Res.* **2019**, *55*, 6896–6910. https://doi.org/10.1029/2019WR025181.
17. Vreča, P.; Gačnik, J.; Žagar, K.; Štrok, M.; Hatvani, I.G.; Kern, Z.; Clement, A.; Milačič Ščančar, R. Isotopic Composition of Precipitation in Small Pannonian Catchments. *Water* **2026**, *18*, 2367. https://doi.org/10.3390/w18192367.
18. Pfahl, S.; Sodemann, H. What Controls Deuterium Excess in Global Precipitation? *Clim. Past* **2014**, *10*, 771–781. https://doi.org/10.5194/cp-10-771-2014.
19. Chen, F.; Zhang, M.; Argiriou, A.A.; Wang, S.; Ma, Q.; Zhou, X.; Wu, X.; Chen, J. Modeling Insights into Precipitation Deuterium Excess as an Indicator of Raindrop Evaporation in Lanzhou, China. *Water* **2021**, *13*, 193. https://doi.org/10.3390/w13020193.
20. Shang, B.; Zhu, G.; Li, T.; Gao, H.; Wang, F.; Zhou, Z.; Fu, T. Global Precipitation d-excess Dataset: A Critical Resource for Geographical Science Research. *Geosci. Data J.* **2026**, *13*, e70043. https://doi.org/10.1002/gdj3.70043.
21. International Atomic Energy Agency (IAEA). Global Network of Isotopes in Precipitation (GNIP). Available online: https://www.iaea.org/services/networks/gnip (accessed on 15 October 2026).
22. Ichiyanagi, K. Review: Studies and Applications of Stable Isotopes in Precipitation. *J. Jpn. Assoc. Hydrol. Sci.* **2007**, *37*, 165–185. https://doi.org/10.4145/jahs.37.165.
23. Barešić, J.; Horvatinčić, N.; Krajcar Bronić, I.; Obelić, B.; Vreča, P. Stable Isotope Composition of Daily and Monthly Precipitation in Zagreb. *Isot. Environ. Health Studies* **2006**, *42*, 239–249. https://doi.org/10.1080/10256010600840226.

24. Argiriou, A.A.; Lykoudis, S. Isotopic Composition of Precipitation in Greece. *J. Hydrol.* **2006**, *327*, 486–495. https://doi.org/10.1016/j.jhydrol.2005.11.053.
25. Chen, L.; Wang, Q.; Zhu, G.; Lin, X.; Qiu, D.; Jiao, Y.; Lu, S.; Li, R.; Meng, G.; Wang, Y. Dataset of Stable Isotopes of Precipitation in the Eurasian Continent. *Earth Syst. Sci. Data* **2024**, *16*, 1543–1557. https://doi.org/10.5194/essd-16-1543-2024.
26. Holmes, J.; Jourdan, A.-L.; Darling, W.G. Stable-Isotope Variability in Daily Precipitation: Insights from a Low-Cost Collector in SE England. *Isot. Environ. Health Studies* **2024**, *60*, 596–614. https://doi.org/10.1080/10256016.2024.2402730.
27. Türk, G.; Gey, C.J.; Schöne, B.R.; Pfister, L. Moisture Origins Affecting Sub-Daily Precipitation $\delta^{18}O$ and d-excess Values Mapped in Western Europe. *Hydrol. Earth Syst. Sci.* **2026**, *30*, 2859–2878. https://doi.org/10.5194/hess-30-2859-2026.
28. Falster, G.; Abramowitz, G.; Hobeichi, S.; Hughes, C.; Treble, P.; Abram, N.J.; Bird, M.I.; Cauquoin, A.; Dixon, B.; Drysdale, R.; et al. High Resolution Monthly Precipitation Isotope Estimates across Australia from Machine Learning. *Hydrol. Earth Syst. Sci.* **2026**, *30*, 289–315. https://doi.org/10.5194/hess-30-289-2026.
29. Gjeshovska, V.; Ilioski, B.; Kovač, Z. Preliminary Results of the Water Isotope Study in the Vardar River Basin, Macedonia. *Water* **2026**, *18*, 1861. https://doi.org/10.3390/w18151861.
30. Gjesovska, V.; Ivanoski, D. Hydrological Analysis of the Upper Vardar River Basin. *Int. Multidiscip. Sci. GeoConf.—SGEM* **2014**, *3*, 157–164.
31. Popovska, C.; Gjeshovska, V.; Ivanoski, D. Floods in Upper Vardar River Basin. In Proceedings of the International Conference on Water Observation and Information System for Decision Support (BALWOIS 2006), Ohrid, Macedonia, May 2006. https://doi.org/10.13140/2.1.2025.8569.
32. Radevski, I.; Hall, J.; Gorin, S.; Petrović, A.M.; Kuzmanoski, A.; Manevska, E.; Ristevski, P. Characteristics of annual and seasonal precipitation in North Macedonia: Change analysis and correlation with the North Atlantic Oscillation (1951–2010). Időjárás 2024, 128, 75–98. https://doi.org/10.28974/idojaras.2024.1.5.
33. Aksoy, E.; Arsov, S.; Mincev, I.; Fang, C. *Agro-Ecological Atlas of the Republic of North Macedonia*; Food and Agriculture Organization of the United Nations (FAO): Rome, Italy, 2020.
34. Gröning, M.; Lutz, H.O.; Roller-Lutz, Z.; Kralik, M.; Gourcy, L.; Pöltenstein, L. A simple rain collector preventing water re-evaporation dedicated for δ18O and δ2H analysis of cumulative precipitation samples. *J. Hydrol.* **2012**, *448–449*, 195–200. https://doi.org/10.1016/j.jhydrol.2012.04.041.
35. Michelsen, N.; van Geldern, R.; Roßmann, Y.; Bauer, I.; Schulz, S.; Barth, J.A.C.; Schüth, C. Comparison of precipitation collectors used in isotope hydrology. *Chem. Geol.* **2018**, *488*, 171–179. https://doi.org/10.1016/j.chemgeo.2018.04.032.
36. Coplen, T.B.; Wassenaar, L.I. LIMS for Lasers for achieving long-term accuracy and precision of δ2H, δ17O, and δ18O of waters using laser absorption spectrometry. Rapid Commun. *Mass Spectrom.* **2015**, *29*, 2122–2130. https://doi.org/10.1002/rcm.7372.
37. Araguás-Araguás, L.; Froehlich, K.; Rozanski, K. Deuterium and Oxygen-18 Isotope Composition of Precipitation and Atmospheric Moisture. Hydrol. Processes 2000, 14, 1341–1355. https://doi.org/10.1002/1099-1085(20000615)14:8<1341::AID-HYP983>3.0.CO;2-Z.
38. Shepard, D. A Two-Dimensional Interpolation Function for Irregularly-Spaced Data. In *Proceedings of the 1968 ACM National Conference*; ACM: New York, NY, USA, 1968; pp. 517–524. https://doi.org/10.1145/800186.810616.
39. Bowen, G.J.; Revenaugh, J. Interpolating the Isotopic Composition of Modern Meteoric Precipitation. *Water Resour. Res.* **2003**, *39*, 1299. https://doi.org/10.1029/2003WR002086.
40. Tian, L.; Yao, T.; MacClune, K.; White, J.W.C.; Schilla, A.; Vaughn, B.; Vachon, R.; Ichiyanagi, K. Stable isotopic variations in west China: A consideration of moisture sources. *J. Geophys. Res. Atmos.* **2007**, *112*, D10112. https://doi.org/10.1029/2006JD007718.
41. Yao, T.; Masson-Delmotte, V.; Gao, J.; Yu, W.; Yang, X.; Risi, C.; Sturm, C.; Werner, M.; Zhao, H.; He, Y.; et al. A review of climatic controls on $\delta^{18}O$ in precipitation over the Tibetan Plateau: Observations and simulations. *Rev. Geophys.* **2013**, *51*, 525–548. https://doi.org/10.1002/rog.20023.
42. Yang, X.; Yao, T. Seasonality of moisture supplies to precipitation over the Third Pole: A stable water isotopic perspective. *Sci. Rep.* **2020**, *10*, 15020. https://doi.org/10.1038/s41598-020-71949-0.
43. Giustini, F.; Brilli, M.; Patera, A. Mapping Oxygen Stable Isotopes of Precipitation in Italy. *J. Hydrol. Reg. Studies* **2016**, *8*, 162–181. https://doi.org/10.1016/j.ejrh.2016.04.001.
44. Machida, I.; Ono, M.; Kamitani, T.; Muranaka, Y. Applicability of d-excess and ^{17}O-excess as groundwater tracers for determination of recharge area. *Hydrogeol. J.* **2022**, *30*, 2027–2041. https://doi.org/10.1007/s10040-022-02526-0.
45. Pang, Z.; Kong, Y.; Froehlich, K.; Huang, T.; Yuan, L.; Li, Z.; Wang, F. Processes affecting isotopes in precipitation of an arid region. *Tellus B Chem. Phys. Meteorol.* **2011**, *63*, 352–359. https://doi.org/10.1111/j.1600-0889.2011.00532.x.

46. Schneck, T.; Telbisz, T.; Zsuffa, I. Precipitation interpolation using digital terrain model and multivariate regression in hilly and low mountainous areas of Hungary. *Hung. Geogr. Bull.* **2021**, *70*, 35–48. https://doi.org/10.15201/hungeobull.70.1.3.
47. Mair, A.; Fares, A. Comparison of rainfall interpolation methods in a mountainous region of a tropical island. *J. Hydrol. Eng.* **2011**, *16*, 371–383. https://doi.org/10.1061/(ASCE)HE.1943-5584.0000330.
48. Field, R.D. Observed and Modeled Controls on Precipitation $\delta^{18}O$ over Europe: From Local Temperature to the Northern Annular Mode. *J. Geophys. Res. Atmos.* **2010**, *115*, D12101. https://doi.org/10.1029/2009JD013370.
49. Palatinuš, I.; Bajo, P.; Briški, M.; Belušić, D.; Brčić, V. Assessing the Influence of Climatic Parameters and Moisture Sources on Precipitation Isotope Composition from Central Croatia: Insights from a Two-Year Long Daily-Resolved Dataset. *J. Hydrol. Reg. Studies* **2025**, *62*, 102836. https://doi.org/10.1016/j.ejrh.2025.102836.
50. Cropper, S.; Solander, K.; Newman, B.D.; Tuinenburg, O.A.; Staal, A.; Theeuwen, J.J.E.; Xu, C. Comparing deuterium excess to large-scale precipitation recycling models in the tropics. *npj Clim. Atmos. Sci.* **2021**, *4*, 60. https://doi.org/10.1038/s41612-021-00217-3.
51. Ciric, D.; Nieto, R.; Losada, L.; Drumond, A.; Gimeno, L. The Mediterranean Moisture Contribution to Climatological and Extreme Monthly Continental Precipitation. *Water* **2018**, *10*, 519. https://doi.org/10.3390/w10040519.
52. Yue, X.; Zhang, M.; Qu, D.; Wang, S.; Chen, F.; Zhang, Y.; Tian, Y. Backward Trajectory Analysis Based on Specific Humidity Correction for the Influence of Moisture Sources on Precipitation Isotopes in the Western Loess Plateau, China. *Water* **2022**, *14*, 3452. https://doi.org/10.3390/w14213452.
53. Wang, S.; Zhang, M.; Hughes, C.E.; Zhu, X.; Dong, L.; Ren, Z.; Chen, F. Factors Controlling Stable Isotope Composition of Precipitation in Arid Conditions: An Observation Network in the Tianshan Mountains, Central Asia. Tellus B Chem. *Phys. Meteorol.* **2016**, *68*, 26206. https://doi.org/10.3402/tellusb.v68.26206.
54. Xia, Z.; Welker, J.M.; Winnick, M.J. The Seasonality of Deuterium Excess in Non-Polar Precipitation. *Glob. Biogeochem. Cycles* **2022**, *36*, e2021GB007245. https://doi.org/10.1029/2021GB007245.
55. Kaseke, K.F.; Wang, L.; Wanke, H.; Tian, C.; Lanning, M.; Jiao, W. Precipitation Origins and Key Drivers of Precipitation Isotope (^{18}O, ^{2}H, and ^{17}O) Compositions Over Windhoek. *J. Geophys. Res. Atmos.* **2018**, *123*, 7311–7330. https://doi.org/10.1029/2018JD028470.
56. International Atomic Energy Agency (IAEA). *Isotopic Composition of Precipitation in the Mediterranean Basin in Relation to Air Circulation Patterns and Climate; IAEA-TECDOC-1453*; International Atomic Energy Agency: Vienna, Austria, 2005. Available online: https://www-pub.iaea.org/MTCD/Publications/PDF/te_1453_web.pdf (accessed on 6 November 2026).
57. Saurer, M.; Kress, A.; Leuenberger, M.; Rinne, K.T.; Treydte, K.S.; Siegwolf, R.T.W. Influence of Atmospheric Circulation Patterns on the Oxygen Isotope Ratio of Tree Rings in the Alpine Region. *J. Geophys. Res. Atmos.* **2012**, *117*, D05118. https://doi.org/10.1029/2011JD016861.
58. Liu, Z.; Bowen, G.J.; Welker, J.M. Atmospheric Circulation Is Reflected in Precipitation Isotope Gradients over the Conterminous United States. *J. Geophys. Res. Atmos.* **2010**, *115*, D22120. https://doi.org/10.1029/2010JD014175.
59. Sha, L.; Tian, L.; Sha, L.; Li, Y.; Wang, X.; Hu, P.; Liang, Q.; Zong, B.; Duan, P.; Cheng, H. Triple Oxygen Isotope Compositions Reveal Transitions in the Moisture Source of West China Autumn Precipitation. *Commun. Earth Environ.* **2024**, *5*, 188. https://doi.org/10.1038/s43247-024-01354-2.
60. Merlivat, L.; Jouzel, J. Global Climatic Interpretation of the Deuterium-Oxygen 18 Relationship for Precipitation. *J. Geophys. Res. Oceans* **1979**, *84*, 5029–5033. https://doi.org/10.1029/JC084iC08p05029.
61. Jia, W.; Xiong, H.; Zhu, G.; Shi, Y.; Zhang, Z.; Yang, L.; Zhang, M.; Zhang, F. Influence of Sub-Cloud Secondary Evaporation and Moisture Sources on Stable Isotopes of Precipitation in Shiyang River Basin, Northwest China. *Water* **2022**, *14*, 2700. https://doi.org/10.3390/w14172700.
62. Wang, L.; Wang, S.; Zhang, M.; Duan, L.; Xia, Y. An Hourly-Scale Assessment of Sub-Cloud Evaporation Effect on Precipitation Isotopes in a Rainshadow Oasis of Northwest China. *Atmos. Res.* **2022**, *274*, 106202. https://doi.org/10.1016/j.atmosres.2022.106202.
63. Kurita, N.; Yamada, H. The Role of Local Moisture Recycling Evaluated Using Stable Isotope Data from over the Middle of the Tibetan Plateau during the Monsoon Season. *J. Hydrometeorol.* **2008**, *9*, 760–775. https://doi.org/10.1175/2007JHM945.1.
64. Kattan, Z.; Nasser, S. Temporal Variability of Precipitation Isotopes in Damascus, Syria—Implications for Regional Climate Change. *Asian J. Atmos. Environ.* **2023**, *17*, 5. https://doi.org/10.1007/s44273-023-00004-x.
65. Hatvani, I.G.; Smati, A.E.; Erdélyi, D.; Szatmári, G.; Vreča, P.; Kern, Z. Modeling the Spatial Distribution of the Meteoric Water Line of Modern Precipitation across the Broader Mediterranean Region. *J. Hydrol.* **2023**, *617*, 128925. https://doi.org/10.1016/j.jhydrol.2022.128925.

66. Natali, S.; Baneschi, I.; Doveri, M.; Giannecchini, R.; Selmo, E.; Zanchetta, G. Meteorological and Geographical Control on Stable Isotopic Signature of Precipitation in a Western Mediterranean Area (Tuscany, Italy): Disentangling a Complex Signal. *J. Hydrol.* **2021**, *603*, 126944. https://doi.org/10.1016/j.jhydrol.2021.126944.
67. Krajcar Bronić, I.; Barešić, J.; Borković, D.; Sironić, A.; Lovrenčić Mikelić, I.; Vreča, P. Long-Term Isotope Records of Precipitation in Zagreb, Croatia. *Water* **2020**, *12*, 226. https://doi.org/10.3390/w12010226.
68. Natali, S.; Doveri, M.; Giannecchini, R.; Baneschi, I.; Zanchetta, G. Is the Deuterium Excess in Precipitation a Reliable Tracer of Moisture Sources and Water Resources Fate in the Western Mediterranean? New Insights from Apuan Alps (Italy). *J. Hydrol.* **2022**, *614*, 128497. https://doi.org/10.1016/j.jhydrol.2022.128497.
69. Borković, D.; Kovač, Z.; Krajcar Bronić, I. Time-Series Analysis of Isotope Composition of Precipitation in Zagreb, Croatia. *Water* **2022**, *14*, 2008. https://doi.org/10.3390/w14132008.

Disclaimer/Publisher's Note: The statements, opinions and data contained in all publications are solely those of the individual author(s) and contributor(s) and not of MDPI and/or the editor(s). MDPI and/or the editor(s) disclaim responsibility for any injury to people or property resulting from any ideas, methods, instructions or products referred to in the content.